March 2020

Model Development to Assess Groundwater Flooding and Levee Underseepage in New Orleans, Louisiana

Shuo Yang
Louisiana State University and Agricultural and Mechanical College

MODEL DEVELOPMENT TO ASSESS GROUNDWATER FLOODING AND LEVEE UNDERSEEPAGE IN NEW ORLEANS, LOUISIANA

A Thesis

Submitted to the Graduate Faculty of the
Louisiana State University and
Agricultural and Mechanical College
in partial fulfillment of the
requirements for the degree of
Master of Science

in

The Department of Civil and Environmental Engineering

by
Shuo Yang
B.S., Jilin University, 2018
May 2020

Acknowledgement

I would like to acknowledge the efforts of all people who helped me in this research. I would like to particularly express my appreciation to Dr. Frank Tsai who provided me the position as a research assistant. He offered a lot of advice and large amounts of research resources during my master program. I'm also very grateful to my other committee members, Dr. Zhiqaing Deng and Dr. Navid Jafari, for their passionate support and suggestions.

In addition, I would like to extend my gratitude to the Department of Civil and Environmental Engineering at Louisiana State University. Excellent professors in the department provide lots of useful courses without which this study cannot be completed smoothly.

Finally, I would like to express my thanks to my friends Dr. An Li, Dr. Jina Yin, Mr. Ye-hong Chen, and Mr. Hamid Vahdat, for their encouragement.

Table of Contents

Abstract

Flooding is a major threat to New Orleans due to its geographic location and geologic condition. However, potential groundwater flooding is seldom studied and poorly understood even though groundwater level is expected high in the city. High groundwater level might result in groundwater flooding in low-lying areas. High uplift pore water pressures may cause strong underseepage and risk levee safety. The objective of this study is to assess the impacts of hydrogeology on groundwater flooding and evaluate potential underseepage-induced hazards along levees in New Orleans. In this study, a groundwater flow model development which involves stratigraphy modeling, groundwater flow model design, sensitivity analysis, model calibration, and uncertainty analysis was conducted in this study. Groundwater flooding was indicated by seepage rate. Underseepage along levees was evaluated by a factor of safety analysis. Parameter uncertainty was incorporated in the assessments of groundwater flooding and levee underseepage. The stratigraphy model showed that 74% of sediments in shallow New Orleans are fine grains. The Pine Island Beach sand along the shore of Lake Pontchartrain is the most pronounced shallow sand in the region. By simulating groundwater flow in 2018, the study found that 40% of New Orleans metropolitan area may have groundwater level 1.0 m above ground surface all year round. The results indicated that relatively severe groundwater flooding comes from well recharged surficial coarse sediments. Residential areas around the Inner Harbor Navigation Canal in the vicinity of Lake Pontchartrain are the most concerned about groundwater flooding, where seepage rate was estimated 4 to 5 mm per day. These areas also exhibit high chance of strong underseepage and potential sand boils. The modeling assessment results agreed well to the IPET's levee assessment for the Hurricane Katrina disaster.

1. Introduction

Risk of flooding in coastal communities increases as global climate changes. Flooding has become more frequent along the coastline in the United States since 1950s, especially in those areas along the Gulf Coast. In addition to surface water, groundwater can be a contributor to the flooding, which is known as groundwater flooding, as sea level keeps rising. Besides, strong underseepage introduced by elevated surface water stage is a potential factor that risks levee safety which can worsen coastal flooding during hurricanes or storm events. The following sections introduce groundwater flooding and levee underseepage, and propose objectives of this study.

1.1. Groundwater flooding

Researchers have assessed the factors that contribute to increasing flooding risks in coastal areas: 1) storm surges associated with hurricanes and storm events with rising sea level, 2) overtopping of levees along rivers and streams due to intensive precipitation or inappropriate management of upstream reservoirs, 3) uncontrolled land development that results in increased run off volume, 4) lacks of efficient stormwater drainage systems, and 5) land subsidence due to groundwater extraction that causes even lower elevation (Adelekan, 2010; Bhat et al., 2013; Rosenzweig et al., 2011). Also, researchers explored coastal flooding issues around the world by modeling approaches. Hydrological models are tools to help identify coastal flooding issues arising from poor drainage designs (Rain et al., 2011), storm surges (Yin et al., 2011), and intensive rainfall with high tides (Zope et al., 2015). However, the contribution of groundwater to flooding (groundwater flooding) has been pointed out.

Groundwater flooding refers to the emergence of groundwater on land surface as a result of groundwater recharge exceeding an aquifer's capacity to store water (Négrel and Petelet-Giraud, 2005). Although flooding from surface water was considered as a major contributor to damages

during hurricanes or storm events, groundwater flooding can be another reason for the destruction of infrastructures (Garcia-Gil et al., 2015). Groundwater flooding rarely causes loss of life, but can last much longer than fluvial flooding depending on local geology, because of groundwater flow velocity is usually lower than surface run off (Morris et al., 2018). Groundwater flooding might always occur, but it didn't attract attentions from scientists until recent a few decades, especially when the United Kingdom suffered from a severe groundwater flooding event in 2001.

Following the devastation of properties associated with groundwater flooding event occurred in the UK, 2001 (Hughes et al., 2011), interest in research about groundwater flooding has been increased in Europe (Ascott et al., 2017; Upton and Jackson, 2011). This event is not the only but the first widespread groundwater flooding in Europe (Morris et al., 2018). The flooding areas are particularly underlain by chalk aquifers. By analyzing observed groundwater levels and soil moisture deficit, Finch et al. (2004) found that high antecedent water table and soil moisture usually coincided with the groundwater flooding events. The shallow chalk aquifers consist of fractured and porous limestone underlain by impermeable limestone. Hydraulic conductivity of these aquifers varies significantly depending on the level of saturation. Micropores retain moisture in unsaturated zones of the chalk aquifers. When the water table is increased above the top of chalk aquifers by intense rainfall, macropores can be filled, which enhances hydraulic conductivity by several order of magnitudes. Then these macropores can hydraulically connect the chalk aquifers with surficial sediments where groundwater discharges as flooding. As the permeability is increased significantly by the filling of macropores, the flooding can occur quickly once the hydraulic connection is established (Pinault et al., 2005). Based on these findings, Adams et al., (2010) developed an early warning system of groundwater flooding from chalk aquifers in the UK. In this system, high antecedent groundwater level coincided with heavy rainfall, coupled with

increasing matric potential, was considered as a trigger to raise the probability of groundwater flooding. Besides, researchers presented several challenges to understand and predict groundwater flooding: 1) it's expensive to obtain extensive data of groundwater levels, stream stages, soil moisture, and precipitations; 2) it's difficult to observe groundwater flooding as it's often masked by precipitations, except for a severe flooding event; 3) groundwater flooding in a region is easy to be influenced by land use and other human activities that are highly uncertain (Macdonald et al., 2008).

After the research about mechanisms of groundwater flooding from chalk aquifers, scientists also realized different groundwater flooding types. Groundwater flooding was classified by the perspectives of causes into three types by Macdonald et al. (2008), researchers from British Geology Survey. The first type of groundwater flooding is caused by the risen water table above land surface in an unconfined aquifer in response to extreme rainfall events. This type of groundwater flooding is often extensive and long-lasting, and corresponds to the flooding event of 2001 in the UK. The second type of groundwater flooding is associated with shallow unconsolidated sedimentary aquifers underlain by relatively impermeable deposits. If these aquifers have good hydraulic connections with surface water, such as rivers, then due to the limited storage capacity of these aquifers, groundwater flooding can come from these aquifers as surface water experiences annual flood seasons. One example is the groundwater flooding in 2002 that caused inundation of large amounts of basements in Dresden, German. This flooding event resulted from high water tables raised by the Elbe River in alluvial aquifers (Kreibich et al., 2009). Severity of the second type of groundwater flooding largely depends on the dynamics of surface water levels. The third type of groundwater flooding results from a reduction of groundwater abstraction which is often associated with industrial activities. The reduction allows depressed water table to

recover, and thus, can cause inundation of subsurface infrastructures, such as basements and tunnels. These research in Europe expanded the knowledge about groundwater flooding and facilitated the recognition of groundwater flooding around the world.

Groundwater flooding events were recorded in the United States. The events that are officially reported occurred in inland areas, including Utah, Colorado, Wisconsin, and Illinois states. For example, groundwater flooding reported in 2008 in Southwest Wisconsin, United States, resulted from significant recharge from intense precipitation (Gotkowitz et al., 2014). Besides, groundwater flooding was recorded in 1993 in Illinois State, which resulted in a groundwater flooding risk map with 100 years return period (Visocky, 1995). Similar to the groundwater flooding event in the UK, the groundwater flooding mentioned above comes from the aquifers that are mainly recharged by precipitation. On the other hand, Macdonald et al. (2012) assessed the risks of groundwater flooding and discussed that groundwater flooding is prone to occur at low-lying areas where groundwater level has strong response to surrounding surface water stage, which corresponds to the second type of groundwater flooding. Such kind of groundwater flooding can be seen along Mississippi River bank in Baton Rouge and urban areas in New Orleans, Louisiana, which is shown in Figure 1. This type of groundwater flooding might also occur in some coastal areas. Groundwater level is expected to be high in coastal cities as sea level keeps rising, which might cause groundwater flooding in some low-lying areas. Hoover et al. (2017) and Rotzoll and Flecher (2013) evaluated the impacts of the rising sea level on groundwater flooding along the coastlines of California and Hawaii, respectively. Potential occurrence of groundwater flooding at some low-lying locations was qualitatively predicted in these studies by analyzing if groundwater head is above land surface. But there is a lack of studies in which groundwater flooding in coastal areas is quantified. This kind of studies can be important to learn

the relationship between geological conditions and the severity of groundwater flooding, and can provide the fundament for control measures and adaptation with respect to groundwater flooding in coastal areas.

(a)

(b)

Figure 1. Groundwater flooding (a) in Louisiana State University Veterinary of Medicine parking lot along Mississippi River bank in Baton Rouge, (b) along Press Drive in New Orleans (from Google Map).

1.2. Levee underseepage

Underseepage is a cause of hazards along levees. Differential hydrostatic head between two sides of a levee occurs when surface water stage is higher than the adjacent land surface. Under

this condition, water can enter pervious stratum through the streambeds and result in piezometric head and hydraulic gradient in the pervious stratum beneath the levee. This groundwater flow is known as underseepage (USACE, 1956). When pore water pressure in the pervious stratum is so strong that exceeds the weight of the overlying top stratum, the top stratum can be lifted by the pressure. The uplift pressure might cause raptures at some weak points of a top blanket, and thus, lead to concentrated upward water flow in the form of sand boils as sands or silts are carried from subsurface to surface. Locations of underseepage and sand boils usually depend on: 1) features of geological unites, such as blankets and underlying sand deposits, and their relations to levees; 2) thickness and hydrogeological properties of the landside top stratum; 3) subsurface holes, cracks, or ditches caused by natural processes, human, or animals. Occurrence of sand boils can be theoretically evaluated by a critical uplift hydraulic gradient value which varies between 0.80 and 0.85 depending on permeability of top stratum (USACE, 1956). Sand boils tend to occur if the uplift hydraulic gradient is greater than the critical value at a location. In addition, even if not causing the uplift of top stratum, strong underseepage can also generate erosive forces which tend to drag soil particles in the pervious stratum. If the erosive forces are greater than resistance forces, then a pipe or tunnel can form as a path of groundwater flow. This process is called piping. Once a piping begins, groundwater flow in the pipe can be enhanced significantly because of the low resistance to flow, which further increases the size of the pipe (Sherard, 1963). Sand boils and piping that are caused by strong underseepage can be potential hazards that impact safety of levees.

Underseepage and associating sand boils or piping were observed in many regions. One striking example is the failures of Mississippi River levee in the Kaskasia Island District of Illinois State in 1993. The failures were caused by sand boils and subsurface piping as the river stage increases to a critical level (Mansur et al., 2000). Based on the data from piezometers in 1993, the

U.S. Army Corps of Engineers (USACE) found that the uplift hydraulic gradients at locations of sand boils are close to the critical value (USACE, 1956). Besides, levees near Yuba City, California, failed in 1986. Sand boils were observed at the toe of the levees before failures while the levees were not overtopped. Furthermore, several sand boils near Mississippi River levee were recorded in Louisiana. In 1975, a sand boil was observed at about 1.6 km away from the levee at the banks of Elbow Bayou. In 1983, a sand boil was developed at the Louisiana State University stadium parking lot which is about 0.8 km from the levee. Several sand boils and excessive pore water pressures were also reported in 1937, 1950, and 1973. These sand boils in Louisiana results from the high water stage in Mississippi River. And these sand boils usually occurs away from the toe of the levee, which was explained by the USACE that thick soil blankets near the levee are sufficient to withstand sand boils but the blankets become thinner away from the levee. In summary, sand boils and piping that are introduced by strong underseepage can influence levee foundations, and even contribute to levee failures. This indicates the importance of control methods of underseepage.

Many measures can be used to control levee underseepage, including riverside blankets, relief wells, landside seepage berms, drainage trenches, and cutoffs (USACE, 1956). Drainage trenches and relief wells aim to release the pore water pressures. Riverside blankets and cutoffs can be used to reduce the seepage from riverside to landside. Landside seepage berms are used to increase the thickness of the top stratum to resist uplift pressures. In general, the combination of several methods is considered to control levee underseepage. The need and selection of control methods should be determined by underseepage analysis.

Underseepage analysis aims to obtain flow net underneath levees and estimate pore water pressure distributions at landside of levees. Traditional underseepage analysis was conducted by

analytical methods. One powerful analytic method is blanket theory (USACE, 1956) which have been widely used for decades by geotechnical engineers. After the advantages of special purpose computer programs for underseepage analysis were presented by Wolff (1989), programs that are based on numerical methods particular for underseepage analysis, such as LEVEEMSU, were developed and employed by researchers. Such programs are powerful when evaluating the performance of underseepage control measures. But these early developed programs simplify levee underseepage as one-dimensional steady-state flow.

Multi-dimensional and temporal underseepage analysis has been a trend in current studies. Many studies about underseepage analysis employed 2D models (Stark et al., 2014), such as SEEP/W, to calculate groundwater head under levees and evaluate risky points with underseepage issues, such as sand boils. Advantages of 2D underseepage models include the relative simplicity of model design and the relative small computation time. However, the utility of 2D underseepage analysis is based on an assumption: the topography, geology, and boundary conditions along the length of the structure are consistent (Cheng et al., 2014). This assumption hardly matches real-world conditions. Thus, 2D models can lead to biased computation of subsurface water pressures. Instead, 3D underseepage analysis can better reflect realistic phenomena. By comparing 2D and 3D underseepage analysis, Jafari et al. (2015) found that the 2D model can underestimate vertical hydraulic gradients and uplift pressures at landside of levees, especially when there are excavations and convex levee (stream) bends. The underestimation can lead to insufficient underseepage control measures. Besides, the importance of transient effects has been pointed out. Flood that can cause strong underseepage usually lasts for a short period during which steady-state flow might not be developed. Under this condition, a transient underseepage analysis that considers the dynamic of boundary conditions and groundwater movement can produce more realistic results.

Stark et al. (2014) compared steady-state and transient models in a case study and found that the steady-state model can overestimate pore water pressures during flood events. Therefore, three-dimensional transient analysis should be preferable when analyzing underseepage and assessing the risks of sand boils or pipings along levees.

Previous research, either employing 2D or 3D underseepage analysis, only focused on specific profiles or small areas containing parts of levees (or dams) (Ahmed and Bazaraa, 2009; Chen and Zhang, 2006; Cobos-Roa and Bea, 2008; Jafari et al., 2015; Stark et al., 2014). These focused profiles or areas might be critical to underseepage issues. But the local models are easy to be biased, which can result from the determination of parameters and landward boundary conditions. Models with different scale can produce variable output (McGlynn et al., 2004). There is a lack of the study that an underseepage model is built in a relatively large area with surrounding natural boundaries, such as surface water and faults, and underseepage along levee systems in the area is analyzed. This kind of study can provide pictures of underseepage issues in regional scales with the accommodation of a variety of factors that can influence the underseepage.

1.3. Objectives

There are two aspects of groundwater flooding and levee underseepage that can be further explored. The quantification of groundwater flooding in coastal areas is needed to reveal the relationship between groundwater flooding and local hydrogeological conditions. A large scale underseepage analysis which takes a variety of factors into account is expected to be conducted. In this study, both of the aspects are expanded by a case study in New Orleans, a low-lying coastal city where flooding was reported over years. The objectives of this study are to: 1) Assess groundwater flooding in New Orleans and explore the impacts of hydrogeology on the potential and severity of groundwater flooding; 2) Perform an underseepage analysis for the entire flood

protection systems in New Orleans, and explore if the large scale analysis can indicate underseepage issues along levees that were not identified or recorded in previous studies. Analyses in this study focused on the year 2018 when no hurricanes or storm events occurred to assess groundwater flooding and levee underseepage in New Orleans in a normal climatic condition. Geology, hydrogeology, the vulnerability of groundwater flooding, and previous levee failures associated with levee underseepage in New Orleans are introduced in section 2. To achieve the objectives, a 3D groundwater flow model in shallow New Orleans was developed using MODFLOW-USG (Panday et al., 2017) based on a large amount of well logs, and was calibrated by groundwater data. The model development process is elaborated in section 3. In section 4, the methods to assess groundwater flooding and levee underseepage are introduced. Section 5 presents results of stratigraphy, groundwater dynamics, seepage, and levee factor of safety in New Orleans. In section 6, features and mechanisms of groundwater flooding were analyzed and underseepage along levees in New Orleans was discussed.

2. Geology, Hydrogeology, and Hazards in New Orleans

Surrounded and intercepted by surface water, New Orleans can be a typical area to study groundwater flooding and levee underseepage. New Orleans is a metropolitan coastal city in southeastern Louisiana, United States, with a population of approximately 1.2 million. The city is adjacent to two coastal lakes: Lake Pontchartrain and Lake Borgne, and is intercepted by Mississippi River. The city also contains several navigation canals, including Inner Harbor Navigation Canal (IHNC), Gulf Intracoastal Waterway (GIWW) channel, Mississippi River Gulf Outlet (MRGO), Harvey Canal and its connecting Intracoastal Waterway (ICW). Besides, three drainage canals which are the 17th Street Canal, Orleans canal, and London Ave Canal were dredged in New Orleans. With the developed navigation systems, New Orleans operates one of the largest ports around the world and contributes to nation's petrochemical industry significantly, so it is important to study groundwater dynamics and identify potential groundwater-induced hazards in the city. Major hazards in New Orleans include urban flooding and land subsidence. These hazards are highly associated with local geological and hydrogeological conditions. Levee underseepage can indirectly contribute to urban flooding, such as the flooding during Hurricane Katrina. Although groundwater flooding is not officially reported in New Orleans, it can potentially occur with continuous subsidence and relatively high surface water stages.

2.1. Urban flooding

New Orleans is vulnerable to flooding due to a number of factors resulting in low effectiveness of natural defenses, including low elevation of much of the city, relatively high stage of surrounding surface water, and land development by reclaiming wetland (Griffis, 2007). Levees were constructed in New Orleans along river, lakes, canals, and waterways to prevent flooding from surface water. The construction of levees made the city isolated so that interior drainage

systems were designed to remove stormwater from rainfall in urban areas of New Orleans (IPET, 2006). However, flooding was reported over years due to heavy precipitation and inefficient pumping of the drainage systems. One of the most severe flooding events occurred in 2005 as Hurricane Katrina hit New Orleans. The high storm surges moved into Lake Borgne and Lake Pontchartrain, then backed up water into drainage and navigation canals in the city (Seed et al., 2008a). The overwhelming stages in these surface water resulted in totally 50 breaches and failures (IPET, 2006) of levees along streams, including IHNC, MRGO/GIWW, the 17th Street Canal, and London Avenue Canal, which led to over 70 percent of the city flooded (ILIT, 2006). Levee failures during Katrina can be partially explained by geological and hydrogeological conditions underneath New Orleans.

2.2. Geology

A review of geological history in coastal Louisiana is presented to better understand shallow geology of New Orleans. The mean sea level 15,000 years ago was about 350 feet lower than current sea level, and the Gulf coastal line was much farther seaward than its current location. The Mississippi River and its distributaries had developed a broad alluvial valley at the Pleistocene surface by entrenching. The width of this valley is about 25 miles and its axis is southwest to New Orleans (Kolb et al., 1975). The rising sea level caused by global warming and glacial melting began to be stable approximately 5000 years ago and was about 5 meters below the current sea level. As a result, drainage channels of the ancestral Mississippi River were inundated, which caused large amounts of fluvial sediments on the broad valley. These sediments can be grouped into two units: a sandy/silty substratum and a fine-grained top stratum. Current deltaic plain was created by these sediments when sea level was stable. Coastal geology of Louisiana is composited by numerous delta systems built by the deposition of Mississippi River sediments (Dunbar and

Britsch, 2008). Five dominant delta systems were formed during the past 7000 years, which are Maringouin, Teche, St. Bernard, Lafourche, and Plaguemines-Balize deltas, from oldest to youngest.

The first major advance of a delta into New Orleans area occurred by the St. Bernard delta system which formed 2000 to 4,000 years ago. The current course of Mississippi River in New Orleans was established by the delta. Dominant distributaries of Mississippi River in New Orleans are the Bayou des Families and the Bayou Metairie-Gentilly systems. The former is south to Mississippi River and extends from west bank of the river; the latter is located north to the river. Both distributaries were active between approximately 700 and 3400 years ago (Frazier, 1967). Mississippi River and the distributaries filled New Orleans with fluvial sediments. With the occurrence of overtopping, overbank deposits from the river and these distributaries formed natural levees. The natural levees with varying thickness are typically formed on the outside of meander loops of the river and along both banks of straight reaches. The natural levees along Mississippi River majorly consists of silty clay and the grain size degrades landward (USACE, 1956). Overbank deposits away from the streams are subsequently transformed into backswamps and marshes. These deposits gradually accumulated in low-lying areas, which eventually formed impervious clay with the thickness ranging from 30 to 80 feet. As those distributaries were abandoned 500 years ago, Mississippi River in New Orleans area turned to the current course. Constructions of the levee along the river prevent other routes from the river to the Gulf. Parts of the Mississippi River levee are underlain by point bars which formed on the insides or convex sides of bends. The point bars consist of silty sand or sand with intervening swales. As the bends grow, point bars are buried by a thin layer of fine-grained materials. The sequence of deposits at

point bar areas tend to grade downward from sandy silt to silty sand and finally to clear sand. The thickness of point bars varies from a few inches to about 25 feet (Kolb et al., 1975).

Descriptions of main shallow geological features in previous literatures are quiet similar and can be summarized: Over half of New Orleans is covered by swamps and marshes consisting of clay and organic matters that usually have low strength depending on water content (ILIT, 2006); the Pleistocene deposits are generally overlain by Holocene fills with the thickness ranging between 55 and 80 feet in New Orleans (Dunbar and Britsch, 2008); high natural levees consisting of clay, silt, and silty sand were formed along the current course of Mississippi River (USACE, 1956); the buried Pine Island Beach Sand stretched along southern shore of Lake Pontchartrain was formed approximately 3,500 years (Saucier, 1963); point bars with downward graded grain size from silty sand to clean sand along parts of the Mississippi River are buried by fine grained materials (Kolb et al., 1975); Metairie-Gentilly ridges and Bayou des Families ridge were old Mississippi River channel fills during the formation of St. Bernard delta (Frazier, 1967).

2.3. Hydrogeology

Some research about hydrogeology in New Orleans has been conducted. According to the study of the U.S. Geological Survey (USGS), there are four principal aquifers, from youngest to oldest, for industrial and commercial use in deep New Orleans, which are Gramercy, Norco, Gonzales-New Orleans, and "1200-foot" aquifers (Dial and Tomaszewski, 1988). Fine-grain aquitards with the thickness varying from a few feet to approximately 200 feet separate each aquifer. In addition to the four aquifers, localized shallow aquifers consisting of point bar sands, distributary channel deposits, and isolated sand beds, exist near land surface. The point bar sands are generally the only shallow permeable deposits that have strong hydraulic connections with Mississippi River (Kolb et al., 1975). The distributary channel deposits refer to sandy fills from

the continuous water flow in a considerable time through the old channels (USACE, 1956). Shallow aquifers occur in a thick relatively impermeable layer overlying Gramercy aquifer. The layer corresponds to backswamps, marshes, and natural levees. Gramercy aquifer with a thickness of about 100 feet has a southward dip and distributes without continuity in the depth between 100 and 300 feet in New Orleans. Norco aquifer is buried between 225 to 500 feet below mean sea level with the thickness ranging from 75 to 135 feet in New Orleans. This aquifer is relatively continuous and pinches out under Lake Pontchartrain. Gonzales-New Orleans aquifer is about 600 feet below mean sea level and has an average thickness of 200 feet (Dial and Tomaszewski, 1988). These aquifers, except for Gonzales-New Orleans aquifer, contain highly mineralized water which is not suitable for human consumption (Eddards et al., 1956). With continuous pumping, Gonzales-New Orleans had been vulnerable to salt water intrusion. Dial and Tomaszewski (1988) developed a three-dimensional groundwater flow model to evaluate the impact of pumping on groundwater level and water salinity in Gonzales-New Orleans aquifer. A four-layer groundwater flow model was also developed by Dial and Sumner (1989) to evaluate New Orleans aquifer systems, including the four principle aquifers, and to predict salt water intrusion with pumping.

In addition to research for deep aquifers, levee underseepage in New Orleans drew more attention from researchers after Hurricane Katrina. Seed et al. (2008b) set up two-dimensional seepage models at two breaches of London Avenue Canal using SEEP/W in order to analyze levee failures mechanisms during Hurricane Katrina. Reasons of severe levee failures along IHNC were also analyzed by two-dimensional seepage simulation by these researchers (Seed et al., 2008c). Moreover, they discussed potential reasons for levee failures along the 17th Street Canal (Seed et al., 2008d). Also, Cobos-Roa and Bea (2008) designed three-dimensional seepage models at the 17th Street Canal and IHNC to analyze the effects of excavation on levee failures. These studies

about levee underseepage in New Orleans suggest mechanisms of main levee failures during Katrina: 1) the failure at northern IHNC in Lower Ninth Ward was caused by highly erodeable lightweight sand fills on embankments while the failure at southern part of IHNC resulted from overtopping of floodwalls; 2) the southern breach along London Ave Canal was caused by underseepage-induced piping and the northern breach was a result of elevated subsurface pore water pressures in underlying sands; 3) the failure at the 17th Street Canal resulted from sliding on the surface of a sensitive organic clayey silt layer that lost shear strength significantly during Katrina. On the other hand, it's reported by Interagency Performance Evaluation Team (IPET) that levee breaches at IHNC, the 17th Street Canal were caused by the instability of clay foundations, while the breaches at London Ave Canal were triggered by I-walls failures founded on sand foundations due to strong underseepage (IPET, 2006). Overall, underseepage plays a considerable role in levee failures during Hurricane Katrina.

In summary, previous studies focused on either groundwater flow in deep confined aquifers or levee underseepage in local areas; however, research about groundwater in shallow aquifers of the entire New Orleans is not seen.

2.4. Subsidence

New Orleans is vulnerable to land subsidence. Subsidence in coastal Louisiana is a result of both natural processes and human activities. Natural processes include compactions and consolidations of deltaic sediments and movement along quaternary faults. Human activities include pumping from aquifers, construction of levees and other flood control structures, dredging of drainage canals (Jones et al., 2016).

Extensive human activities have caused severe subsidence in New Orleans area. For one thing, constructed levees along Mississippi River prevent new fluvial sediments being introduced

to floodplain and low-lying areas during flood seasons of the river. Another, engineered structures on levees can contribute to compactions and consolidations of levee foundations, which can cause local subsidence (Dunbar and Britsch, 2008). Furthermore, drainage canals were dredged to dewater marshes and swamps as land development was required due to the ever-increasing population after World War II. The drop of water table in organic sediments facilitated compactions and oxidations of organic matters, which resulted in an extensive decline of surface elevation. Dewatering of shallow aquifers and pumping from Gonzales-New Orleans aquifer were believed to be the dominant drivers of severe subsidence in New Orleans by Jones et al. (2016). Metropolitan areas in New Orleans suffered from an average subsidence rate of about 8 mm per year during 2002 to 2005. The most severe subsidence of over 20 mm per year occurred in east New Orleans. Fifteen (15) percent of land in New Orleans was reported to be about 10 feet lower than mean sea level in 2006. These land areas are between Lake Pontchartrain and Mississippi River, and are covered by marshes and swamps (ILIT, 2006). Severe subsidence has caused an interior basin adjacent to the southern shore of Lake Pontchartrain (Snowden et al., 1980).

As New Orleans keeps sinking due to continuous dewatering, pumping, and the lack of introduction of new sediments, the city can be exposed to not only catastrophic fluvial flooding risks but also high groundwater level and pore water pressure.

2.5. Potentials of groundwater flooding and levee underseepage

Hydrogeology and subsidence indicate the potentials of groundwater flooding and levee underseepage in New Orleans. As a coastal city surrounded by levees, continuous subsidence make surface water stage higher and higher relative to land surface in New Orleans. The large gradient can result in high groundwater level in shallow aquifers, especially those connected with surface water, such as point bar sediments. The high groundwater level might contribute to the occurrence

of groundwater flooding, which might worsen urban flooding and impact subsurface infrastructures. Besides, strong underseepage along levees introduced by the large difference between land surface and surface water stages can be another concern in New Orleans. The underseepage might cause sand boils and piping, and risk levee safety. While many research about levee underseepage has been conducted (mentioned in section 2.3), these studies only focused on the parts of levees that failed during Katrina. Other areas with potential underseepage issues cannot be reflected in these studies.

In brief, previous studies are not enough to understand groundwater flooding and levee underseepage in New Orleans. A research about the groundwater flow in shallow aquifers of the entire New Orleans city is the key to learn these two issues. Therefore, it's important to explore groundwater level dynamics in New Orleans and identify risky areas with groundwater-induced hazards.

2.6. Study area

To learn groundwater flooding and levee underseepage in New Orleans, the study area should capture as much as surface water as possible. In this study, the study area covers the entire New Orleans metropolitan area, containing parts of four parishes: Orleans, Jefferson, St. Bernard, and Plaquemines. The study area is bounded by Lake Pontchartrain to the north, Lake Borgne and a part of Mississippi River to the east, Lake Salvador and Barataria Water Route to the south, and Duncan Canal to the west (Figure 2). The study area also includes IHNC, GIWW, MRGO, Harvey Canal, ICW, and three drainage canals. As Mississippi River passes through, most of the study area is encircled by levees and surge barriers. Low-lying land surface coupled with relatively high stages of surface water around and within the study area makes it a representative area to study groundwater flooding and levee underseepage.

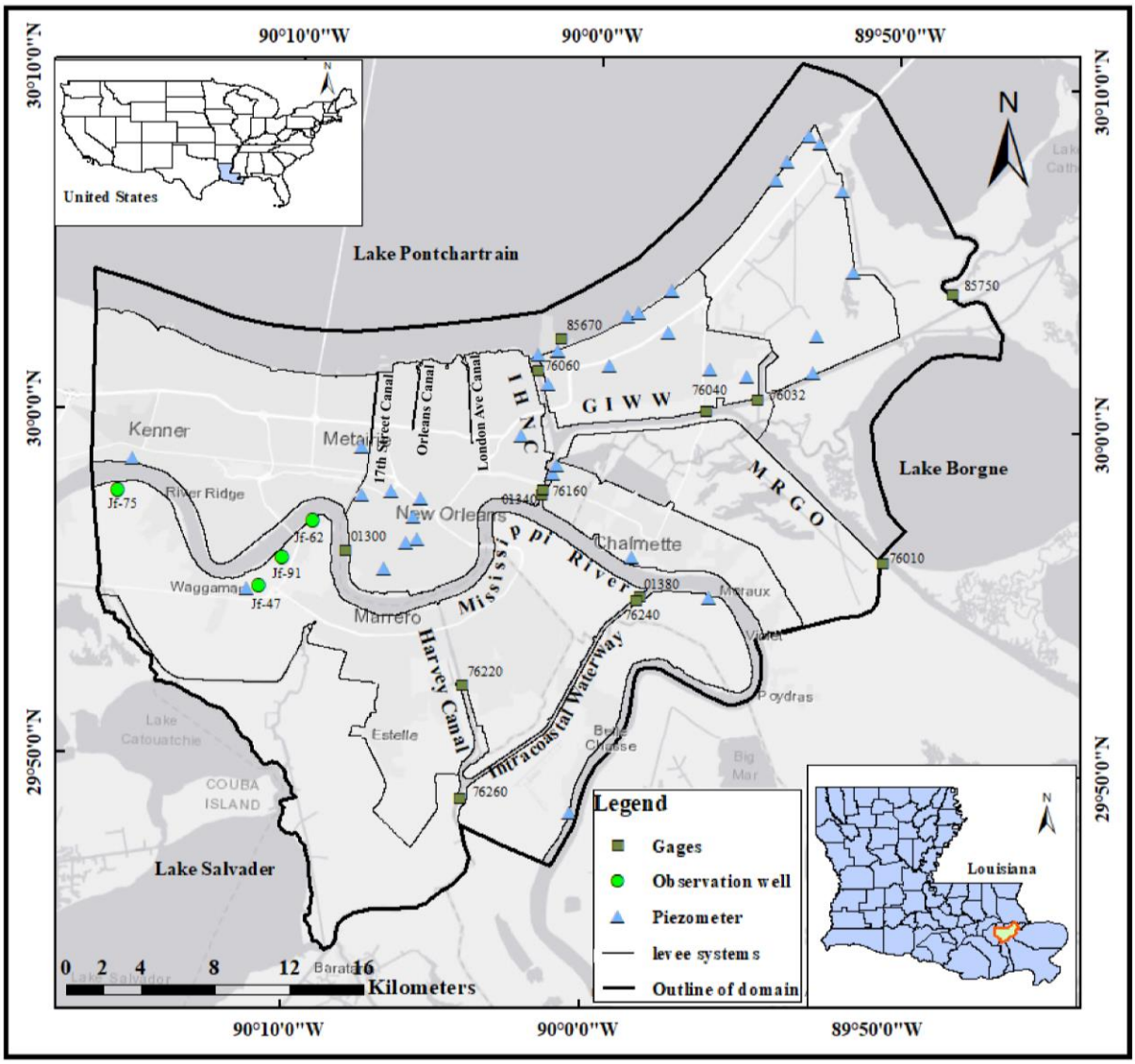

Figure 2. Study area of Greater New Orleans is delineated. Name of surface water, locations of shallow piezometers, observation wells, and gages are displayed. Two gages are out of the map. The basemap is from Esri ArcGIS.

3. Groundwater Flow Model Development

In this study, the groundwater flow model development involves data collection, stratigraphy modeling, groundwater flow model design, sensitivity analysis, model calibration, and uncertainty analysis. A stratigraphy model was constructed to learn the topography and shallow geology of the study area. Then a groundwater flow model was designed based on the stratigraphy. A sensitivity analysis was conducted to evaluate the significance of parameters in the groundwater flow model. The parameter significance is used for model calibration. Finally, an uncertainty analysis was performed to learn the variability of the model output by incorporating the parameter uncertainty. The following sections introduce general concepts of these procedures and elaborate the particular methods employed in this study.

3.1. Data collection

There are four types of data used in this study: well log data, topographic data, surface water stage data, and monitored groundwater level data.

Geotechnical borings and drillers' logs (well log data) were collected from Louisiana Department of Natural Resources (LDNR), the Coastal Protection and Restoration Authorities of Louisiana (CPRA), and the USACE. There are 2873 logs data located within and nearby the study area. The data is in form of manual records which contain locations of boreholes, construction time, sediment descriptions (sediment type, size of grains, and color) at each depth interval. Lithologic information in each well log was interpreted into 4 sediment groups and 11 sediment classes (shown in Table 1). The organized data can be used to explore soil distribution underneath the study area.

Topographic data derives from a Digital Elevation Model (DEM). DEM is an array of elevation data referenced to a coordinate system. The DEM used in this study that includes the

elevation of both land surface and stream valleys in the study area is generated by Love et al. (2010). The high-resolution DEM has the cell size ranging from 10m to 30m and is referenced to the vertical tidal datum of North American Vertical Datum of 1988 (NAVD 88).

Table 1. Sediment groups and sediment classes in well log interpretation.

Sediment group	Sediment class
Sand	Sand, silty sand, clayey sand
Silt	Sandy silt, silt, clayey silt
Clay	Sandy clay, silty clay, clay, organic clay
Organic	Peat

Table 2. Gages in each surface water. LP: Lake Pontchartrain.

Name	ID	Stream
Mississippi River at Bonnet Carre	01280	Mississippi River
Mississippi River at New Orleans (Carrollton)	01300	Mississippi River
Mississippi River at IHNC Lock	01340	Mississippi River
Mississippi River at Aligiers Lock	01380	Mississippi River
Mississippi River at Alliance	01390	Mississippi River
Inner Harbor Navigation Canal (IHNC Lock) New Orleans	76160	IHNC
Seabrook Bridge - Inner Harbor Nav Canal	76060	IHNC
GIWW near Paris Road Bridge	76040	GIWW
IHNC Surge Barrier West / Protected Side	76032	GIWW
Harvey Canal Sector Gates North / Protected	76220	Harvey Canal
GIWW at West Closure Complex Protected Side	76260	Harvey Canal
Algiers Lock - GIWW	76240	ICW
Lake Pontchartrain at Lakefront Airport	85670	LP
Chef Menteur Pass nr Lake Borgne	85750	Chef channel
Bayou Dupre Sector Gate - East/Flood Side	76010	Lake Borgne

The surface water stage data of Mississippi River, IHNC, GIWW, Lake Pontchartrain, Lake Borgne, Harvey canal, and ICW in the study area is from the gages of USACE. Locations and names of these gages are shown in Figure 2 and Table 2, respectively, which include 5 stream gages along the Mississippi River, 4 stream gages for IHNC and GIWW, 1 stream gage for Lake Pontchartrain, 1 stream gage for Harvey canal, 2 stream gages for ICW, 2 stream gages for Lake

Borgne. Daily water stage data after 1986 can be found from USACE's website (http://rivergages.mvr.usace.army.mil/).

Discontinuous groundwater level data in New Orleans was recorded by the USGS in 1950s and 1960s. Locations of observation wells are shown in Figure 2. These four types of data was used for the groundwater flow model development.

3.2. Stratigraphy development

An investigation of subsurface processes, such as groundwater flow and environmental hazards, usually require a detailed and realistic definition of subsurface geology, which are usually achieved by geological modeling. In this section, some popular geological modeling methods are reviewed. Also, the development of a multiple indicator natural neighbor (MINN) interpolation method and its application to construct the stratigraphy in this study are introduced.

3.2.1. Geological modeling

Geological modeling is a common method to learn big pictures of geological structures with local known information (Turner, 2006). Geological modeling usually involves two steps: 1) establishing a geometry model; 2) analytical computation to determine geological characteristics inside the geometry with known data. Many geological modeling techniques have been used to explore subsurface conditions. Electrical Resistivity Tomography (ERT) is a popular geophysical technique to detect shallow geology. ERT aims to measure subsurface electrical resistivity using electrodes, and image the 2D or 3D profiles of subsurface structures by solving inverse problems. ERT has been applied with great success in geological and hydrogeological characterization (Negri et al., 2008). Apart from ERT, borehole-based geological modeling methods, most of which are based on interpolation, have been developed in recent years. For example, Clay Fraction (CF) modeling is a method to create a 3D geological model with borehole data. The output of a CF

model is the clay percentage in each voxel (Foged et al., 2014). Also, Calcagno et al. (2008) constructed a geological model by developing the potential-field interpolation which can interpolate geological features between boreholes using locations of the geological interfaces and orientation data. In general, the development of geological models using widely spaced borehole data requires reliable interpolation methods which can be variable depending on data features.

3.2.2. Multiple indicator natural neighbor interpolation

A multiple indicator natural neighbor (MINN) interpolation method was developed to explore sediment distribution underneath New Orleans in this study. The MINN technique is based on the natural neighbor (NN) interpolation method (Green and Sibson, 1978; Sibson, 1980, 1981) which has been applied to identify parameter structures in geophysical parameterization problems (Tsai et al., 2005). The following three paragraphs introduce NN interpolation method, the development of MINN interpolation method, and the application of MINN method in this study, respectively.

NN interpolation is a robust and reliable method to construct a surface with irregularly distributed sample points. NN interpolation does not require specified parameters, such as numbers of neighbors in nearest neighbor interpolation, to support operations. Those parameters subjectively specified by users can result in variable interpolation results. In contrast, NN interpolation can derive sample points and their weights automatically from the geometric properties of input dataset for each query point. The core of NN interpolation is Dirichlet Tessellation which is also known as Voronoi Diagram (Dirichlet, 1850; Voronoi, 1908). Only one Voronoi Diagram can be generated given a set of sample points, which means NN interpolation is stable and consistent. NN interpolation process can be easily understood with Figure 3. In a NN interpolation process, after the generation of Voronoi Diagram with sample points (Figure 3(a)), a

query point would be inserted into the diagram. Then a new polygon including the query point can be created in the structure. Each neighbor polygon contributes to the area of the new polygon (Figure 3(b)). Samples inside in these neighbor polygons are defined as natural neighbors (Sibson, 1981). These natural neighbors are used to compute the value at the query point. Weight of each sample is proportional to the area contributed by each neighbor polygon to the new polygon. NN interpolation can be formulized by the following:

$$\hat{z}(u) = \sum_{i=1}^{N} \frac{a_i}{A} \times z_i \tag{1}$$

where, $\hat{z}(u)$ is the value calculated at a query point with the coordinate of u; N is the total number of natural neighbors for the given query point; a_i refers to the area contributed by the polygon where the i^{th} natural neighbor falls (Figure 3(b)); A is the total area of the new polygon; z_i is the sample value of the i^{th} natural neighbor. Based on NN interpolation, a MINN approach was developed for the interpolation of categorical data in this study.

The idea of MINN interpolation is to perform NN interpolation at one query point for several times to obtain the probability of occurrence of each categorical value at the query point. The categorical value is defined as the indicator. Only one indicator is focused in each NN interpolation. When a new polygon where a query point falls is created in the Voronoi Diagram, the natural neighbors around the new polygon are assigned with binary values. The natural neighbors having the focused indicator are assigned with 1; other natural neighbors not having the focused indicator are assigned with 0. Then the result of this NN interpolation is a numeric value between 0 and 1 at the query point. The numeric value corresponds to the probability of occurrence of the focused indicator at the query point. The NN interpolation at the query point can be repeated for other indicators. Finally, the sum of probabilities of occurrence of indicators at each query

point would be one. The categorical value produced by MINN interpolation at one query point is determined by the indicator with the largest probability of occurrence at the query point.

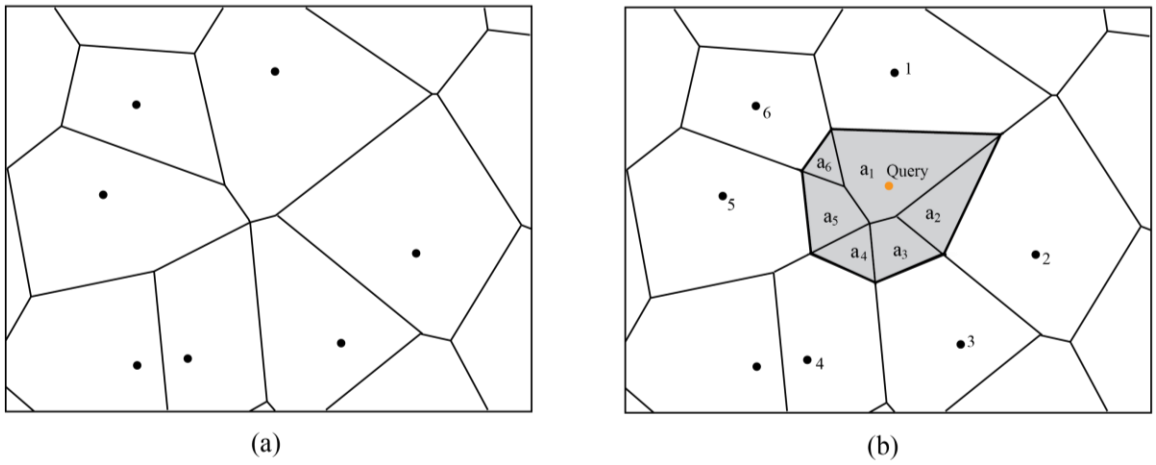

Figure 3. Illustration of natural neighbor interpolation. (a) Generated Voronoi Diagram with sample points. (b) Contribution of areas by the original diagrams to the new polygon created after the insertion of a query point. The new polygon is shown with grey color. Natural neighbors are noted with numbers.

In this study, with the topobathymetry derived from a DEM, MINN interpolation was performed with logs data to construct a stratigraphy model in New Orleans. Horizontal geometry of the stratigraphy model is the same as the domain outline shown in Figure 2. The well logs data is the sample point in MINN interpolation. The indicators in this case refer to the sediment classes in the logs data (Table 1). And query points are densely distributed in the domain. Figure 4 displays the locations of logs in the study area and the percentile of their bottom elevation ranges. Well logs are mainly distributed in metropolitan area encircled by flood protection systems, while less data is available in undeveloped zones in the eastern and southwestern study area that are covered by wetland. 76.2 % logs' bottom is higher than El. -50 ft (-15 m); 17 % logs have bottom deeper than El. -200 ft (-61 m), and some of them extend to the depth of over 2000 ft (609 m). However, it's not necessary to construct a deep stratigraphy model, because the aim of this study is to analyze groundwater flooding and levee underseepage which are highly correlated with shallow aquifers.

Therefore, a stratigraphy model extending to El. -200 ft (-61 m) was developed above which an adequate amount of sediment information is available.

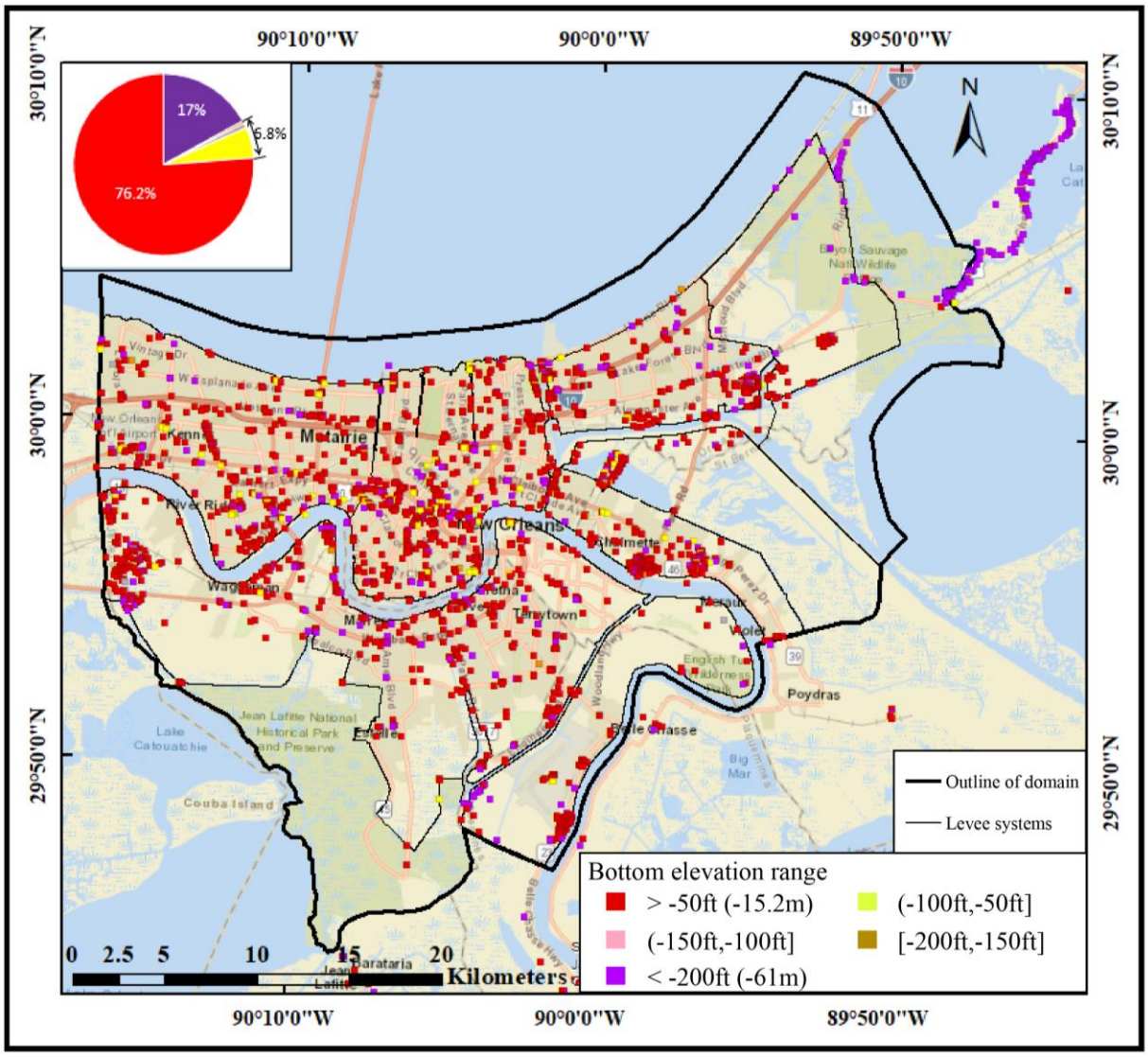

Figure 4. Location of well logs in the study area. Colors correspond to the range of bottom elevation (NAVD 88) of logs. The pie graph shows the fraction of bottom elevation ranges of well logs. The basemap is from Esri ArcGIS.

3.3. Groundwater flow model design

Groundwater flow modeling was employed as a tool to learn groundwater level distribution in the study area. In this sections, different types of groundwater flow models are introduced, and the groundwater flow model design using MODFLOW-USG is focused.

3.3.1. Groundwater flow models

Groundwater flow modeling is proved to be an efficient tool for learning aquifer's response, and thus, evolve appropriate groundwater management strategies, as a groundwater flow model can be a simplified version of real system which simulates all of parameters describing significant characteristics of aquifers (Thangarajan, 2007). A groundwater flow model can be either used for predicting aquifer's future behaviors or learning dynamics of groundwater systems. There has been various groundwater flow modeling techniques since 1900s which can be classified into three types: physical models, analog models, and mathematical models.

Physical models, which are also known as sand tank models, were widely employed during 1930 to 1950. This technique can learn aquifers' response in a field scale by simulating the groundwater flow in a laboratory scale. Materials (usually sand with different grain size) that reflect aquifers' hydraulic properties can be introduced into a tank. Simulations can be performed with pumping from the model and appropriate boundary conditions (Thangarajan, 2007). But physical models for groundwater flow simulation can be expensive and time-costing. Analog models became more prevalent than physical models after 1960s.

Dominant analog modeling techniques for groundwater flow simulation in a regional scale are viscous fluid models and electric analog models (Prickett, 1975). The idea inside viscous fluid models is that the viscous liquid flow between two parallel plates can be an analog of groundwater flow in aquifers (Hele-Shaw, 1897). The key of electric analog models is that groundwater flow can be analogous to the flow of electric current in conductors. This technique builds an analogy between Darcy's law and Ohm's law. In the models, hydraulic conductivity is analogized to electrical specific conductivity. These two types of analog models can be used to simulate groundwater flow in continuous medium.

Mathematic models can be either stochastic or deterministic. Stochastic models can be used to obtain solutions based on probabilities of occurrence, and are widely used when analyzing flooding risks. Deterministic models are based on relationships between known events and systems, and are generally used to handle issues associated with groundwater. Deterministic models can be classified into analytical models and numerical models. Analytical models are used to obtain an exact solution of mathematical equations. However, groundwater flow equations in real-world conditions are so complicated that might not be directly solved by analytical techniques. In general, assumptions and simplifications, especially for boundary conditions, are required to make calculations feasible. Analytical models are usually used for in-situ field test to estimate parameters. Numerical models aim to obtain an approximation rather than an exact solution by solving partial differential equations (PDE). In groundwater hydrology, the PDE refers to the following groundwater flow governing equation:

$$\frac{\partial}{\partial x}(K_x \frac{\partial h}{\partial x}) + \frac{\partial}{\partial y}(K_y \frac{\partial h}{\partial y}) + \frac{\partial}{\partial z}(K_z \frac{\partial h}{\partial z}) = S_s \frac{\partial h}{\partial t} + W \quad (2)$$

where, h is groundwater head; t is time; K is hydraulic conductivity in x, y, and z directions; S_s is the specific storage; W is source or sink item. Finite difference and finite element methods are important numerical approaches to solve the PDE (Thangarajan, 2007). In finite element method, the continuous pore medium is divided into a number of small-volume elements. Groundwater head and hydrogeological properties are consistent in each element. The key of finite element method is to transform the governing equation (2) into integral form and perform integration over the elements. One advantage of this method is that it can define boundary conditions easily because shape of the elements is flexible. But this method is usually computationally intensive (Thangarajan, 2007). In the finite difference method, a continuous porous medium is represented by a bunch of discrete points which are called nodes. Each node is assigned with parameters.

Therefore, difference operators defining relationships between parameters can replace partial derivatives. Then, each node have one finite difference equation. Solving these finite difference equations is an iterative process. There are many algorithms based on finite difference method developed to solve equation (2). One of the most popular algorithms around the world is the modular three-dimensional finite difference groundwater flow model which is known as MODFLOW (Macdonald and Harbaugh, 1988).

3.3.2. MODFLOW-USG

MODFLOW is a computer code that solves three-dimensional groundwater flow equation in multi-layer porous medium based on finite difference method. The source code was written primarily by FORTRAN in 1980s. The first version released by USGS is MODFLOW-84. The latest version is called MODFLOW 6, while MODFLOW-2005 is still widely used by scientists around the world. MODFLOW allows transient groundwater flow to be simulated in both confined and unconfined aquifers. Apart from a main program, MODFLOW also contains a number of modules based on object-oriented design. These modules are also known as packages, such as drain package and river package, which can be easily used or changed by users and programmers. In 2000, MODFLOW was expanded by an addition of code, which is called groundwater flow (GWF) processes, that solves groundwater flow equations containing a set of underlying packages. Many graphical user interfaces (GUI), such as ModelMuse and GMS, were developed to help users design groundwater flow models with these packages.

MODFLOW-USG is one of specialized versions of MODFLOW. It uses unstructured-grid method to simulate groundwater flow. Normal versions of MODFLOW only allows rectangular grid which might not fit well with irregular model boundaries. In contrast, MODFLOW-USG allows both structured and unstructured grid types, such as triangular, rectangular cells, or grids

with other shapes. This improvement makes grids easily follow the shape of boundaries. Besides, MODFLOW-USG has more flexibility in grid design compared to normal versions of MODFLOW. For example, MODFLOW-USG can be used to improve resolution only in areas of significance, such as rivers and wells. MODFLOW-USG is developed based on an underlying control volume finite difference (CVFD) formulation which allows a cell to connect with an arbitrary number of other cells. To better implement CVFD method, the groundwater flow governing equation is rewritten as equation (3):

$$\int (K\nabla h)\cdot ndS = S_s V\frac{\partial h}{\partial t} + WV \tag{3}$$

where, S is the surface of the control volume; n is an outward-pointing normal vector on the volume surface. The CVFD method requires certain geometrical properties of cell connections. This requirement can be violated by irregular cell geometry, which can introduce errors to simulation results. Accuracy of CVFD formulation for grids with irregular shapes is improved using a generalized Ghost Node Correction (GNC) package (Panday et al., 2013). Moreover, MODFLOW-USG includes connected linear network (CLN) process. Groundwater flow can be simulated between CLN grids and GWF grids. The term of CLN segment, which refers to connected CLN cells, is used in MODFLOW-USG. CLN segments can be used to represent wells and drain. CLN segments can also be combined together to represent a network, for example, when simulating groundwater flow in karst conduits.

In brief, unstructured grids and flexible connections between cells in MODFLOW-USG make it feasible to construct a groundwater flow model in a domain with irregular shape and to refine cells in areas of interest. Coupled with CLN process, MODFLOW-USG can be a powerful tool to construct complicated groundwater flow models.

3.3.3. Model design

The stepwise processes for groundwater flow modeling with numerical methods generally include conceptual model, mathematical model, model design, model calibration or verification (Baalousha et al., 2008). The conceptual model of a domain is expected to be developed before designing a groundwater flow model. Sediment properties, sink and source terms, boundaries, and other necessary data for simulation should be defined in the conceptual model. One appropriate mathematical model should be selected depending on the conceptual model to solve groundwater flow equations. Model design is the conversion from a conceptual model to a grid model, in which parameters (including hydrogeological properties, initial conditions, and boundary conditions) of each grid are properly assigned. Model calibration is the process that parameters in a groundwater flow model is adjusted to make simulation results close to real-world phenomena as much as possible.

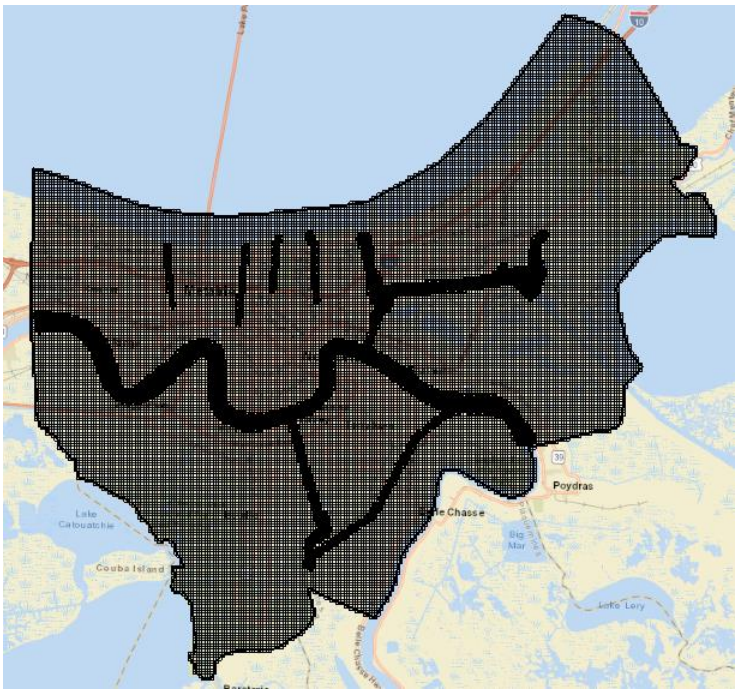

Figure 5. Discretization of one layer in the groundwater flow model. The areas of Mississippi River, IHNC-GIWW, the 17th Street Canal, Orleans Canal, London Ave Canal, and Harvey Canal-ICW are refined. The basemap is from Esri ArcGIS.

A relatively complicated groundwater flow model was designed to explore groundwater's response to surface water stage in the study area. The stratigraphy model which includes sediment distribution, topography, bathymetries of surface water, and boundaries can be used as a conceptual model. The 11 sediment classes in the stratigraphy were divided into 4 groups, i.e. sand, silt, clay, and organics (Table 1), and sediment classes in each group have similar hydrogeological properties. Thus, the groundwater flow model was developed with the four sediment types. The model domain (Figure 2) with irregular shape contains some surface water with small areas, such as IHNC and GIWW, which requires local high-resolution grids. Therefore, MODFLOW-USG was employed as a mathematical model in this study. MODFLOW-USG has the flexibility of having finer meshes around Mississippi River, major canals and waterways while keeping a coarser mesh for the model domain. Grids of the model was designed in GMS. The base cell size is 200m × 200m, while cells at the bathymetries of Mississippi River, IHNC, GIWW, Harvey canal, and ICW were gradually refined to 50 m×50 m to better capture the coarse grains distribution at bathymetries. Grids of one layer is shown in Figure 5. As a result, there are 24 layers and 68,492 cells for each model layer.

Boundaries conditions and initial conditions of the model were assigned after the generation of grids. The initial condition of groundwater head was determined by a steady-state solution. Edges of the model were given as no flow boundaries. Cells in areas of surface water were assigned with general head boundaries (GHB). GHB package is available in MODFLOW-USG. The package assigns flow rate into a boundary based on the difference between external source water heads and groundwater heads in boundary cells:

$$Q = \frac{k}{l} A(H - h) \tag{4}$$

where, Q is the flow rate into boundaries; k refers to the permeability of streambeds and l is the thickness of streambeds; k/l is called leakance of streambeds and needs to be estimated or calibrated; A is the area that is expected to directly contact with surface water on a cell surface; H and h refer to external source water head and groundwater head in GHB cells, respectively. GHB cells in the model were identified by localizing cells at bathymetry of each surface water in the DEM. And A of each GHB cell was computed by summing up areas of the GHB cell faces adjacent to the space of valley. There are four separate GHB in the groundwater flow model: Mississippi River, IHNC-GIWW, Harvey Canal-ICW, and Lake Pontchartrain-Lake Borgne. These GHB areas are shown in Figure 6. The separation is based on connections between surface water. Surface water connected together is combined as one boundary. Each GHB has independent leakance of streambeds. The k/l and A for each GHB cell are fixed after calibration while external source water heads (H) in each GHB cell is subject to change depending on simulation period.

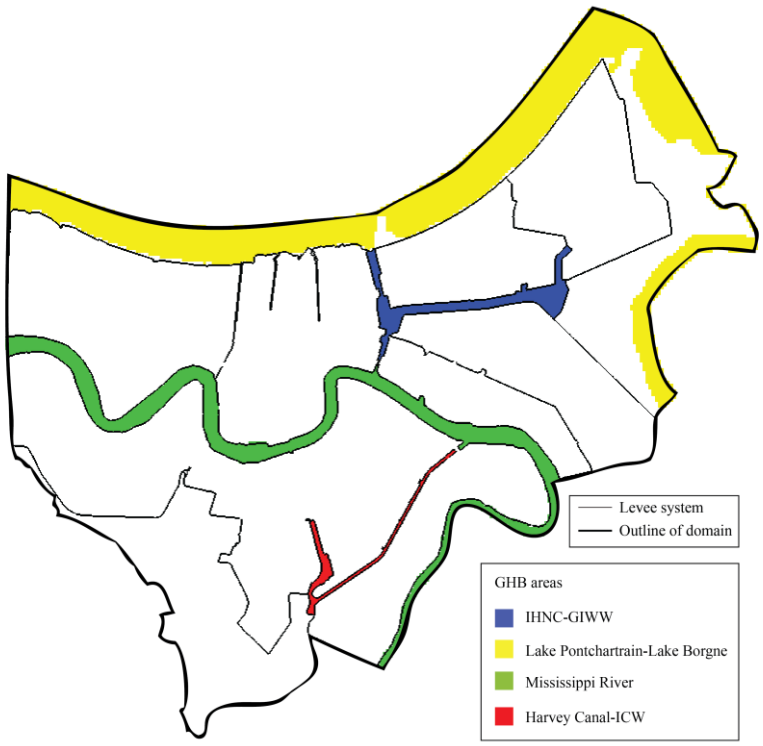

Figure 6. Four GHB areas in the groundwater flow model.

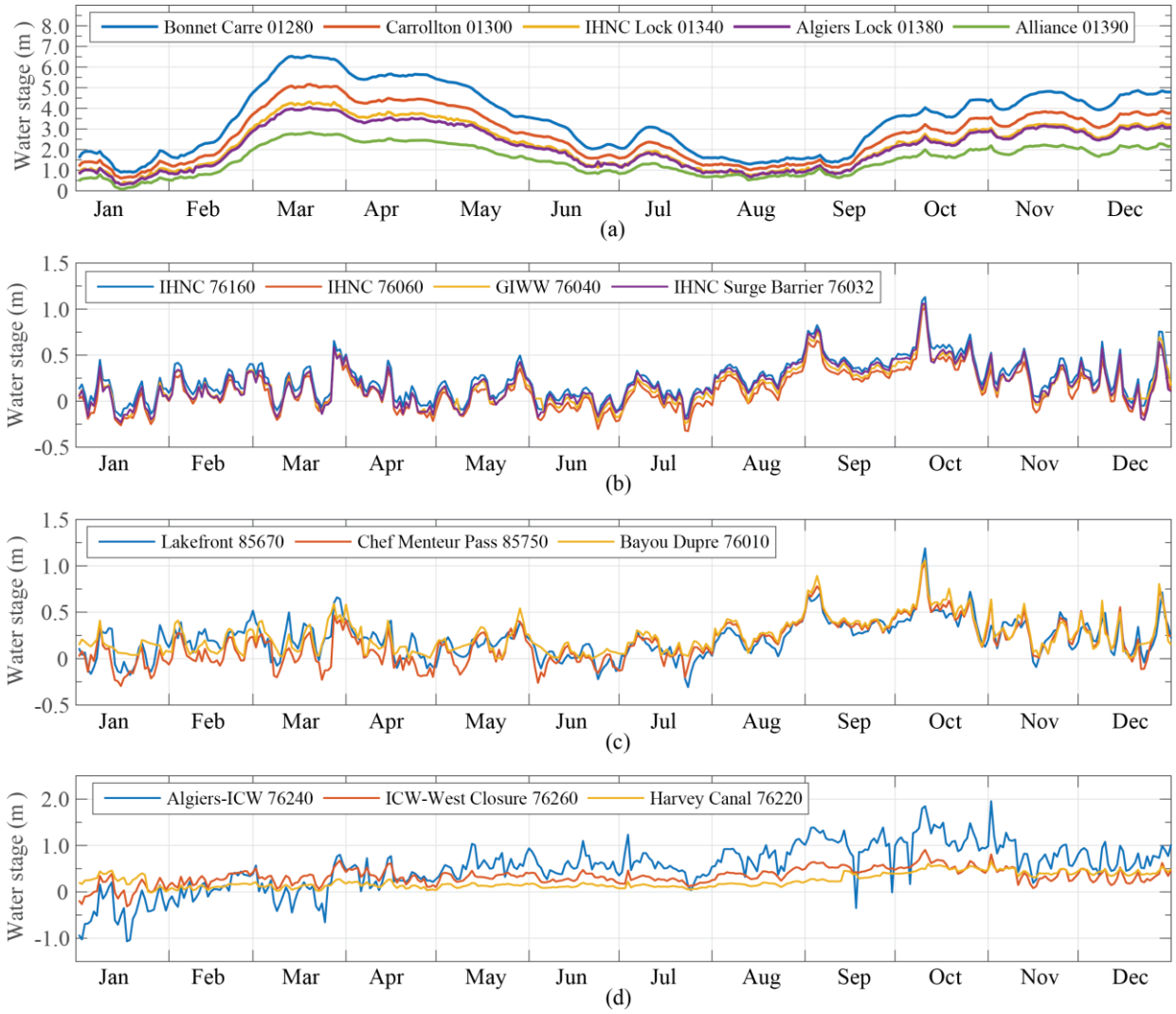

Figure 7. Hydrographs in 2018 at gages of (a) Mississippi River, (b) IHNC and GIWW, (c) Lake Pontchartrain and Lake Borgne, and (d) Harvey Canal and Intracoastal Waterway (ICW). Water stage is relative to NAVD 88.

As this study focuses on the groundwater flow in the year 2018, the methods to determine the water head (H) in GHB cells in each GHB area are based on the features of surface water stage in 2018. The hydrographs in 2018 at gages in each GHB areas are shown in Figure 7. As the stretched and meandering Mississippi River intercepting the study area results in over 3 meters difference in river stage between upstream and downstream during the flood season in 2018 (Figure 7(a)), water head of GHB cells at the bathymetry of Mississippi River was assigned with interpolated values from 5 gages (shown in Table 2) along the river. First of all, linear interpolation

of water stage was performed using the gages as sample points and cells along the two river banks as query points. Then, water stage in all GHB cells at the bathymetry of Mississippi River was interpolated with inverse distance weighted approach using cells along river banks as sample points. While apparent differences in recorded water stage of gages at IHNC, GIWW, Harvey canal, and ICW are not observed (Figure 7(b), (d)), water head of GHB cells in these surface water was assigned with mean stage value of respective gages. Each of Lake Pontchartrain, Lake Borgne, and the connecting channel (Chef Menteur Pass) only has one gage (Figure 7(c)). As the three surface water is connected and water stage differences among the three gages are no more than 0.5 meter in 2018, water head of GHB cells in the three surface water was given as an average stage value of the three gages. Besides, dynamics of surface water stage was considered in GHB. In each stress period, GHB cells at which water head doesn't exceed their top elevation (dry cells) were assigned with the conductance of zero, which means water would not entry from these cells.

Hydrogeological properties in each cell was assigned according to the sediment class at corresponding location in the stratigraphy model. Each sediment group (Table 1) in the stratigraphy model was assigned with an indicator. Sand, silt, clay, and organic has an indicator of 1, 2, 3, and 4, respectively. In the conversion from the stratigraphy to the grid model, each cell was assigned with an indicator that represents one sediment group. Therefore, hydrogeological parameters, including hydraulic conductivity, anisotropy, specific storage, and specific yield, in each cell can be assigned according to the indicator.

3.4. Sensitivity analysis

A groundwater flow system is influenced by many factors associated with hydrogeological settings. It's not easy to learn how much these factors impact the system. Sensitivity analysis is an effective tool to reveal underlying relationships between these factors and the groundwater flow

system inside a groundwater flow model (Zeng et al., 2012). In this section, various sensitivity analysis approaches are reviewed, and composited scaled sensitivity which was employed in this study is focused.

3.4.1. Techniques for sensitivity analysis

Many sensitivity analysis techniques have been developed. Sensitivity analysis generally can be classified into two categories: global sensitivity analysis and local sensitivity analysis. Global sensitivity refers to the sensitivity of various results that the one model is able to output by exploring all possible parameter ranges. In global sensitivity analysis, the impact of one parameter on a model output is averaged on both the probability distribution of the parameter and the probability distributions of all other parameters (Saltelli et al., 1999). Global sensitivity analysis can be further classified into regression-based, derivative-based, variance-based, and moment-independent sensitivity analysis (Janetti et al., 2019). Local sensitivity analysis focuses on local influence of variables on output and is suitable when investigating specific points of interest. In local sensitivity analysis, partial derivative of model outputs with respect to a parameter is calculated to estimated sensitivity around nominal value of the parameter. The sensitivity can be estimated by finite-difference derivative, direct differentiation, and adjoint differentiation methods (Slooten et al., 2010). Compared to local sensitivity analysis, global sensitivity can measure the contribution of not only single model parameter but also a set of parameters to the variability of model outputs.

Sensitivity analysis techniques have been performed to estimate influence of parameters on groundwater flow systems. General purposes of sensitivity analysis includes 1) identification of model parameters with limited impact on model outputs, 2) ranking of model parameters according to their relative contribution to variability of model outputs, and 3) providing

information of parameter probabilistic distributions (Janetti et al., 2019). Rajabi et al. (2015) used moment-independent methods to obtain parameter uncertainties in a seawater intrusion model. Deman et al. (2015) conducted regression-based sensitivity analysis on groundwater lifetime expectancy. Chen et al. (2018) employed a surrogated-based method to calculate parameter importance in a groundwater flow model. Dai et al. (2017) also applied a variance-based approach to evaluate uncertainties derived from conceptual models. Above all, sensitivity analysis is a powerful tool to assess parameter influences and quantify parameter uncertainties in a groundwater flow model.

3.4.2. Composited scaled sensitivity

The purpose of sensitivity analysis in this study is to estimate parameter significance to simulated groundwater head. And the evaluated significance is used to select parameters for model calibration. Locations of observation wells are primarily of interest in this study. Therefore, the sensitivity analysis technique that can effectively compare sensitivities among different parameters is needed in this study. Composited scaled sensitivity (CSS) is one of the statistics measuring the amount of information provided by data. It is generated by the nonlinear regression model UCODE, a computer program used to solve weighted least-square problems with modified Gauss-Newton method. The CSS calculates a dimensionless model parameter sensitivity to a set of simulated groundwater heads at selected locations (e.g., observation locations or locations of interest). Thus, CSS is able to compare the influences of parameters on simulation results. CSS can be calculated as follows (Ely, 2006):

$$\frac{\partial h_i}{\partial b_j} = \frac{h_i(b_j + \Delta b_j) - h_i(b_j)}{\Delta b_j} \tag{5}$$

$$CSS_j = \sqrt{\frac{1}{n}\sum_{i=1}^{n}\left(\frac{\partial h_i}{\partial b_j}\frac{b_j}{\sigma_i}\right)^2} \tag{6}$$

where, $\partial h_i/\partial b_j$ is the local sensitivity of groundwater head using forward-difference derivative for the model parameter; Δb_j is the change of the j^{th} parameter value; $h_i(b_j)$ and $h_i(b_j+\Delta b_j)$ refer to the simulated groundwater head with the parameter value of b_j and $b_j+\Delta b_j$, respectively; CSS_j is the CSS of the j^{th} parameter by summarizing sensitivities among n simulated groundwater head data; σ_j refers to standard deviation of groundwater head with different values of the parameter.

In this study, parameters involved in sensitivity analysis includes hydraulic conductivity (K), specific storage (S_S), specific yield (S_Y) of four sediment types, and leakance of each streambed (parameter in GHB package of MODFLOW-USG). Most piezometers in the study area are used to monitor groundwater head at deep confined aquifers, such as Gonzales-New Orleans aquifer. Piezometers in shallow aquifers of New Orleans are quite limited. 34 piezometers (shown in Figure 2) in shallow aquifers identified by the LDNR were used by industries. However, no groundwater data are available from industrial piezometers. Only four USGS piezometers (noted as observation wells in Figure 2) along Mississippi River have available groundwater data recorded in 1957-1962. Generally, large CSS values indicate influential parameters with respect to simulated groundwater heads at selected locations (Hill, 1998). Therefore, CSS was calculated at locations of the four USGS observation wells. The information of parameter importance provided by the calculation can be useful in the model calibration. CSS is also computed at locations of the totally 38 wells to reflect to influence of each parameter on groundwater head in shallow aquifers of New Orleans. The CSS values were scaled between 0 and 1 for comparison.

3.5. Model calibration

Groundwater flow model output is expected to accurately match the real-world conditions as much as possible. However, model parameters, such as hydraulic conductivity, measured either in field or laboratory might not contribute to the simulated values that match well with

observations. This discrepancy comes from not only inevitable errors in measurements but also scale effects. Under these conditions, model calibration is introduced to reduce the difference between simulated values and observed values. Model calibration is the process that the model construction and parameters are adjusted to make the model output reasonably fit with the realistic phenomena. In this study, the model calibration was achieved via inverse modeling using an optimization technique.

3.5.1. Inverse modeling

One of the most common approaches to achieve model calibration is inverse modeling. Inverse modeling refers to the methods to estimate parameter values given a number of observations. The advantages of inverse modeling approach includes 1) determination of reasonable parameter values that contribute to the best possible fit with observations, 2) quantification of calibration quality with statistical measures, 3) illustration of predictive performance with parameter estimations, and 4) identification of model limitations, such as structures of geological units (Poeter and Hill, 1997).

One common method based on inverse modeling is trial-and-error method. In this method, the model parameters are assigned to perform the simulation. The simulation results, such groundwater heads, are compared with observed values. Then the model parameters are adjusted to produce a better fit between the simulation results and observations. This process is repeated until a desirable match is obtained. The trial-and-error method can be preferable if the model is relatively simple and contains a small number of parameters.

On the other hand, parameter estimations based on inverse modeling can be achieved by optimization techniques which have been widely used to calibrate groundwater flow models. The aim of the optimization is to minimize difference between observations and model output. So the

weighted least-square objective function is usually used to formulate the problem. This nonlinear minimization problem is usually solved by a modified Gauss-Newton method (Hill, 1998) which generally has a good performance. In this method, the gradient of an objective function is computed to determine the direction in parameter domain to reduce the objective function. This algorithm converges when the gradient equals to or is close to zero. Therefore, Gauss-Newton method is capable of searching the local minimum rather than the global minimum of the objective function, because a groundwater model can be highly complicated and lead to an objective function with multiple local minimum. The method can produce different solutions with variable starting points. Besides, evolutionary algorithms (EA) can be used to solve the optimization problem and produce global minimum. One popular algorithm from EA family is genetic algorithm (GA). In GA, a population of candidate solutions of an optimization problem is evolved to better solutions. The EA family also includes Covariance Matrix Adaptation Evolution Strategy (CMAES), Differential evolution, etc. Performance of techniques can be variable when applied to different optimization problems (Arsenault et al., 2013). In brief, techniques to solve objective functions for model calibration are not unique, and selection of techniques should depend on specific conditions, such as simulation time, performance of techniques, etc.

3.5.2. Optimization-based calibration

In this study, calibration of the groundwater flow model can be formulated as a least square problem which can be solved by optimization methods. The objective of the problem is to minimize the root mean square error (RMSE) between simulated groundwater heads and observed heads:

$$RMSE = \sqrt{\frac{1}{L}\sum_{i=1}^{L}(h_i(p) - h_i^{obs})^2} \tag{7}$$

where, L is the number of observations; $h_i(p)$ and h_i^{obs} represent the simulated groundwater head with an array of parameters p and the observed groundwater head, respectively, at the i^{th} observation. Parameters significant to groundwater heads at observation wells determined by sensitivity analysis can be involved in the calibration process, and other parameters can be assigned with median of respective reference values from previous literatures. Parameters involved in the calibration were constrained by reasonable intervals to reduce iterations for convergence and produce realistic results. EA might be an option to solve the optimization problem, but EA usually require large amounts of simulations to get desirable solutions. For instance, large population size is required by GA to enhance the possibility to get desirable minimum. Each individual in the population should be evaluated by one simulation. In this study, each simulation of the groundwater flow model costs at least one hour depending on parameter values, which makes the convergence extremely time-consuming. This means that evolutionary algorithms are not suitable for the above optimization problem.

Instead, the optimization problem was solved by sequential quadratic programming (SQP) approach which is widely used to solve constrained nonlinear optimization problems (Boggs and Tolle, 1995; Boggs and Tolle, 2000; Nocedal and Wright, 2006). SQP is based on a profound theory and can provide powerful algorithms to solve optimization problems. Consider one nonlinear optimization problem with the following form:

$$\begin{aligned} &Min && f(x) \\ &Subject\ to && z(x) = 0, g(x) \le 0 \end{aligned} \tag{8}$$

where, $f(x)$ is the objective function; $z(x)$ and $g(x)$ describe equality and inequality constraints, respectively. By replacing the objective function $f(x)$ with its local quadratic approximation and replacing the constraint functions $z(x)$ and $g(x)$ with their local affine

approximations, the above nonlinear optimization problem can be converted to a quadratic programming (QP) subproblem with the form:

$$\begin{aligned} &\textit{Min} && \nabla f(x^k)^T (x - x^k) + \frac{1}{2}(x - x^k)^T \nabla^2 f(x^k)(x - x^k) \\ &\textit{Subject to} && z(x^k) + \nabla z(x^k)^T (x - x^k) = 0 \\ & && g(x^k) + \nabla g(x^k)^T (x - x^k) \le 0 \end{aligned} \tag{9}$$

where, $\nabla f(x)$ is the gradient of the objective function; $\nabla^2 f(x)$ is the Hessian of the objective function. SQP is an iterative process which solves a QP subproblem for a given iterate x^k and then uses the solution to construct a new iterate x^{k+1}. Finally, the sequence of x can converge to a local minimum of the original nonlinear optimization problem. Optimization toolbox with SQP algorithm in MATLAB was employed to solve the optimization problem in this study (MathWorks, 2015). To achieve the automatical calibration of the groundwater flow model, the model was linked with MATLAB toolbox by developing a MATLAB function in which model parameters p are input and simulated groundwater heads at observations $h_i(p)$ are output.

3.6. Uncertainty analysis

Uncertainty analysis is an important process in modeling. Once uncertainty analysis is conducted, confidence level of model output can be described by statistical measures and effects of the limitations of models can be identified (Geffray et al., 2019). In this study, uncertainty analysis aims to quantify the variability of the groundwater flow model output introduced by uncertain model parameters. Many techniques were developed for propagations of uncertainty, including Monte Carlo simulation, differential analysis, response surface methodology (RSM), fast probability integration (FPI), etc. Helton and Davis (2003) summarized and compared many techniques for uncertainty analysis, and pointed out that Monte Carlo simulation is generally the

most effective technique to provide propagation and analysis of uncertainty. In this section, Monte Carlo simulation is introduced and its application in this study are particularly focused.

3.6.1. Monte Carlo simulation

Monte Carlo simulation is a powerful technique to solve random problems and provide global approximation of uncertainty. Monte Carlo simulation is based on the selection of the model input from probability distributions. General procedures of Monte Carlo includes: generating random input data (samples) from a probabilistic distribution, running models (calculations) with the generated data, collecting output, and repeat (Chin et al., 2013). Thus, a random problem is converted to many deterministic problems that are easy to solve. The precise of the output can be evaluated by the variability of the output resulting from the random samples using statistical procedures (Bekesi and McConchie, 1999). The advantages of implementing Monte Carlo simulation can be summarized: 1) uncertainties can be extensively explored with appropriate samples; 2) modification of the model is not required; 3) distributions of the model output can be directly obtained. The most important procedure of Monte Carlo simulation is sampling.

Many sampling techniques for Monte Carlo simulation have been developed. One of the simplest techniques is random sampling. This method excludes correlations between variables. Therefore, random sampling cannot assure that samples can be generated from any subsets of the sample space. In some conditions, subsets with low probability but large significance are easy to be missed. Stratified sampling can solve this problem by specifying subsets of domain from which samples are generated. In stratified sampling, the domain of variables are divided into large amounts of separate subsets. Probability of each subset is calculated. Then a sample set is generated by sampling from each subset. However, the calculation of subset probabilities becomes challenging when the sample domain has high dimensionality.

Latin Hypercube Sampling (LHS) is a compromise between random sampling and stratified sampling. LHS was proposed by Iman and Conover (1980), and is believed to be able to generate representative variable values with a small sample size (Florian, 1992; Huntington and Lyrintzis, 1998). Like random sampling, LHS is a probabilistic procedure. Similar to stratified sampling, LHS involves division of a domain of variables, but the probabilities of subsets are not required to be computed. LHS can not only generate samples for each variable that represents its probability distribution but also consider correlations between variables. In LHS, the cumulative distribution function (CDF) of one variable is divided into many equal intervals depending on the number of samples, and only one sample is selected randomly from each interval. For high dimensional LHS samples, each variable in a sample is generated independently and randomly combined together. After generating samples, LHS can order the samples to take correlations between variables into account (Iman and Conover, 1982). LHS has been employed extensively for propagation of uncertainty of complex systems in many fields. Ayyub and Lai (1989) coupled LHS with variance reduction techniques to assess structural stability. McKay (1992) incorporated LHS as a tool to perform uncertainty analysis of computer models. LHS was also used to generate training data for system reliability assessment (Metya et al., 2017). The growing use of LHS indicates its power for uncertainty propagation and its role in Monte Carlo simulation.

3.6.2. Implementation of Monte Carlo simulation

In this study, due to the limited observed data, uncertainty analysis is expected to be conducted to produce more reliable model output and learn the impact of parameter uncertainties on simulation results. Only four USGS observation wells with 20 observed groundwater head data are available for calibration in the study area. And these observation wells are distributed in a concentrated manner (Figure 2). Therefore, the simulated groundwater head around these

observation wells after calibration can be relatively accurate, while there is no assurance of accuracy of simulated groundwater head in other areas away from the observation wells. This indicates the importance of uncertainty analysis in this study.

Monte Carlo simulation was employed to achieve the uncertainty analysis. Large amounts of simulations are expected to be performed in Monte Carlo simulation to capture cases as many as possible, which is computationally intensive, especially for highly complicated models with large numbers of variables. In this study, computational expense was reduced by improving sampling effectiveness. The sampling ranges of parameters involved in the model calibration was narrowed by a linear statistical approach (Bard, 1974):

$$Cov = \frac{1}{L-M}\sum_{i=1}^{L}(h_i - h_i^{obs})^2[J^T J]^{-1} \tag{10}$$

where, L the number of observations; M is number of parameters involved in the sampling. J represents L × M Jacobian matrix in which each row contains the sensitivities of one observation to M parameters. A Multi-Gaussian distribution of parameter values can be obtained with the calculated covariance matrix Cov using parameter values determined by calibration as the mean. Besides, the linear statistic method was not implemented to other parameters not involved in the model calibration because this method cannot narrow the ranges of these parameters for sampling. Groundwater head at observation wells usually have small sensitivities with respect to those parameters not involved in the model calibration, which can make the calculated variance (using the linear statistic method) of these parameters extremely large. The large variance can result in the samples that exceed reasonable ranges. Therefore, parameters not involved in the model calibration are expected to be sampled from uniform distributions of reference values. Some methods have been developed to reduce sample size, such as spectral representation approach (Shinozuka and Deodatis, 1991) and auto-regressive moving average (ARMA) technique

(Samaras et al., 1985). However, most of these methods are developed for specific cases, and don't extensively work well. In this study, Latin hypercube sampling (LHS) which is able to generate representative variable values with a small sample size was employed. Samples generated from the Multi-Gaussian distribution and the uniform distributions are combined to perform Monte Carlo simulation. The variabilities of simulated groundwater heads at observations with regard to parameter uncertainties are quantified. To produce a more reliable analysis, parameter uncertainties were considered by performing Monte Carlo simulation when analyzing groundwater level dynamics, groundwater flooding and levee underseepage.

4. Methods to Groundwater Flooding and Levee Underseepage Assessments

This section introduces the methods to analyze groundwater flooding and levee underseepage. In this study, groundwater flooding was considered as seepage which can be quantified by Darcy's law. The severity of levee underseepage and its relating hazards (sand boils) in the study area was evaluated by a factor of safety analysis. The following sections elaborate these methods.

4.1. Seepage calculation

Groundwater flooding rate was rarely calculated previously. Groundwater flooding extent was usually measured by aerial photography (Finch et al., 2004). Due to the absence of extensive groundwater level information, areas exposed to groundwater flooding were predicted using monitored groundwater level data (Macdonald et al., 2012). Moreover, groundwater head contour and DEM were used to identify the areas with potential occurrence of groundwater flooding in a regional scale without considering the severity of groundwater flooding at specific locations (Hoover et al., 2017). But the quantification of groundwater flooding is important to learn the relationship between local hydrogeology and groundwater flooding.

In this study, groundwater flooding was reflected by seepage rate which can be estimated by Darcy's law (Darcy, 1856). Darcy's law is an equation that formulates the flow of fluid through a porous medium. Darcy's law is based on experiments that the flow of water through a column filled with sand is observed. Darcy's law provides a strong fundament in hydrology and hydrogeology. One application of Darcy's law is to formulate the groundwater flow in aquifers. Darcy's law can describe the relationship among groundwater flow rate, hydraulic conductivity, and hydraulic gradient. In this study, Darcy's law can be written as the following form:

$$Q = -K \frac{\partial h}{\partial z} A \tag{11}$$

where Q is the seepage rate in the area of A that is typically the size of each surficial cell in the groundwater flow model; K is the hydraulic conductivity of surficial sediments; $\partial h/\partial z$ refers to the upward hydraulic gradient at surficial cells. The upward hydraulic gradient is defined as difference of groundwater head between a unit distance in the vertical direction. It can be calculated using the simulated groundwater head from the groundwater flow model. The equation (11) can reflect several properties of seepage (groundwater flooding): 1) seepage occurs from high groundwater head points to low groundwater head points; 2) no seepage occurs if there is no upward hydraulic gradient over a distance; 3) The greater the hydraulic gradient, the larger the seepage rate if the hydraulic conductivity is constant. Darcy's law is applicable only for laminar flow which can be evaluated by Reynolds number:

$$\mathrm{Re} = \frac{\rho v d_{30}}{\mu} \tag{12}$$

where, ρ is the density of the fluid; ν refers to the specific discharge which is the flow velocity through an area of medium; d_{30} is a representative grain size of the porous medium; μ is the dynamic viscosity of the fluid. For one type of fluid flowing in a homogeneous medium, the larger the specific discharge, the larger the Reynolds number. In general, the flow with the Reynolds number no more than one is considered as laminar flow. To apply Darcy's law for seepage calculation, it is assumed that seepage is a slow and continuous process in this study.

4.2. Factor of safety analysis

Underseepage analysis is an important approach to learn levee underseepage and its potential impacts on levees. Groundwater that enters into the pervious sediments overlain by impervious stratum along levees would create an artesian pressure, and high pressure might result in heaving and sand boils at landside areas. Factor of safety (FS) analysis has been widely used in geotechnical engineering to evaluate soil state relative to some critical conditions, which is often

associated with underseepage issue. The FS analysis is a simple and reliable method to reflect underseepage-induced hazards, slope stability, etc., with the accommodation of parameter uncertainties. Therefore, FS was used as an index for risks of geohazards along levees in this study. FS against uplift was specifically used to identify the risky areas with severe underseepage and associating potential sand boils along levees in New Orleans. FS against uplift at points of interest can be computed using the simulated groundwater head and the information from stratigraphy (Cheng et al., 2014):

$$FS = \frac{i_c}{i_v} = \frac{i_c}{(H_b - H_t)/B} \tag{13}$$

where, i_c is the critical gradient required to result in uplift of top stratum and is determined by the ratio of the unit weight of the soil in top stratum to the unit weight of water, theoretical value of i_c for clay and silt top stratum is 0.8 and 0.85, respectively (USACE, 1956); i_v represents vertical hydraulic gradient; H_b refers to the groundwater head at substratum; H_t is the total hydraulic head at land surface; B is the thickness of the top stratum. Two assumptions should be made when using equation (13): 1) groundwater flow through the top stratum is vertical and in the underlying pervious stratum is horizontal; 2) groundwater flow is laminar.

The thickness of the top stratum is of great importance in the FS analysis. The thickness can be obtained from the stratigraphy model developed in this study. While the top stratum hardly consists of one single material but usually composed of several different sediment layers, the thickness of the top stratum is expected to be transformed into equivalent effective thickness by the following equation:

$$L_t = L_{\text{int}} \frac{K_{imp}}{K_l} \tag{14}$$

where, L_t is the transformed thickness of a layer; L_{int} represents the actual thickness of the layer; K_{imp} refers to the hydraulic conductivity of the most impervious layer (usually refers to clay) in the top stratum; K_l is the hydraulic conductivity of the layer to be transformed (USACE, 1992). The effective thickness of the top stratum is equal to the thickness of the least pervious layer plus the transformed thicknesses of more pervious layers. Thus, effective thickness would equal to L_{int} where the top strata only consists of the least pervious sediments.

5. Results and Discussions

The results of the groundwater flow model development, including stratigraphy, sensitivity analysis, model calibration, and parameter uncertainty are presented and discussed in section 5.1~5.3. Parameter uncertainty is incorporated in the groundwater flow simulation in 2018. In section 5.4, shallow groundwater level dynamics of New Orleans in 2018 is discussed. The results of the assessments of seepage in urban areas and levee factor of safety are presented in form of maps in section 5.5 and 5.6. Section 5.7 focuses on the discussions of groundwater flooding mechanisms and levee underseepage in New Orleans.

5.1. Stratigraphy

The New Orleans shallow geological features in the stratigraphy model are similar to previous studies (ILIT, 2006). Surficial sediments distribution in New Orleans is shown in Figure 8. 74 percent of soil in the stratigraphy consists of fine grains (clay, silty clay). Figure 8 shows that 88.2 percent of New Orleans is covered by clayey and silty sediments. 10.1 percent of the city is covered by sandy deposits, and 1.7 percent is covered by organic matters. Coarse sediments (sand and silty sand) distribute at parts of bathymetries of Lake Pontchartrain, Mississippi River, IHNC, and GIWW. The Pine Island Beach Sand (Saucier, 1963) is pronounced along the shore of Lake Pontchartrain.

The sediment distribution in cross sections is displayed in Figure 9. The cross section AA' and BB' illustrate a beach sand layer with the thickness of about 10 meters along the shore of Lake Pontchartrain in the northeastern New Orleans. This beach sand layer corresponds to the Pine Island Beach described by Saucier (1963). As shown in the cross section CC', the western reach of the beach sand extends to the area close to the 17th Street Canal. Besides, the cross section AA' and BB' show a sand layer with the thickness ranging between 25 to 30 meters underneath the

beach sand. This thick sand layer is a part of Gramercy aquifer. The annotation of Gramercy aquifers in cross sections (Figure 9) are according to Dial and Sumner (1989). Lake Borgne and the connecting channel are covered by fine grains. Also, the cross section AA' illustrates the connections of GIWW with not only sandy deposits but also organic matters (organic clay and organics). The cross section BB' indicates the connection between ICW and sandy deposits. Moreover, clay, sandy clay and silty clay distribute in the top stratum along Mississippi River and compose natural levees. All of the cross sections in Figure 9 indicate that buried point bars contact parts of Mississippi River with varying thickness and elevations, especially at the river bends. These point bars consist of various sediment classes, including sand, silty sand, sandy silt, and sandy clay, which matches the descriptions of geology in New Orleans by Kolb et al. (1975). Apart from the coarse grains connecting with surface water, isolated sand beds are displayed in the cross section CC', DD', and EE'. The sand beds are parts of shallow aquifers in New Orleans (Dial and Tomaszewski, 1988). In the stratigraphy model, connections between shallow aquifers (coarse-grained sediments) and surface water in New Orleans can be observed between: point bar sands and Mississippi River, the Pine Island Beach sand and Lake Pontchartrain together with IHNC, GIWW and organic matters, and surficial sands and ICW.

In addition, topography and bathymetry (shown in Figure 10) in New Orleans is obtained from the stratigraphy. The highest areas in New Orleans are artificial levees along Mississippi River with the elevation up to 8.4 meters (NAVD 88). The elevation of natural levees along the river varies between 1 to 3 meters. Abandoned Mississippi River distributaries are also reflected in Figure 10. A west-east ridge and a north-south ridge are located at the northern and southern side of Mississippi River, respectively. The former ridge corresponds to the Metairie-Gentilly-Sauvage system and the latter corresponds to the Bayou des Families ridge. Locations of these

ridges match well with those in the geology map presented by Dunbar and Britsch (2008). Sediment fills along the abandoned distributaries are 0.5 to 1.5 meters in elevation. Besides, 47.3 percent of the land in New Orleans is below mean sea level (NAVD 88). And Figure 10 shows apparent low-lying areas in front of Lake Pontchartrain, which is also illustrated in cross sections BB', CC', and DD' (Figure 9). The land over 3 meters lower than mean sea level in the area east to IHNC, partially because of the subsidence resulting from the dewatering (extraction of shallow groundwater) during land development (Jones et al., 2016; ILIT, 2006). Moreover, Figure 10 shows that the lowest location of the Mississippi River channel with the elevation of -59.4 m (NAVD 88) occurs at a river bend. The deepest streambed in IHNC and GIWW has the elevation of about -11 m. The elevation of Lake Pontchartrain and Lake Borgne beds vary from -2.5 m to -5 m, except for the bathymetry with the lowest elevation of about -14 m adjacent to IHNC and drainage canals.

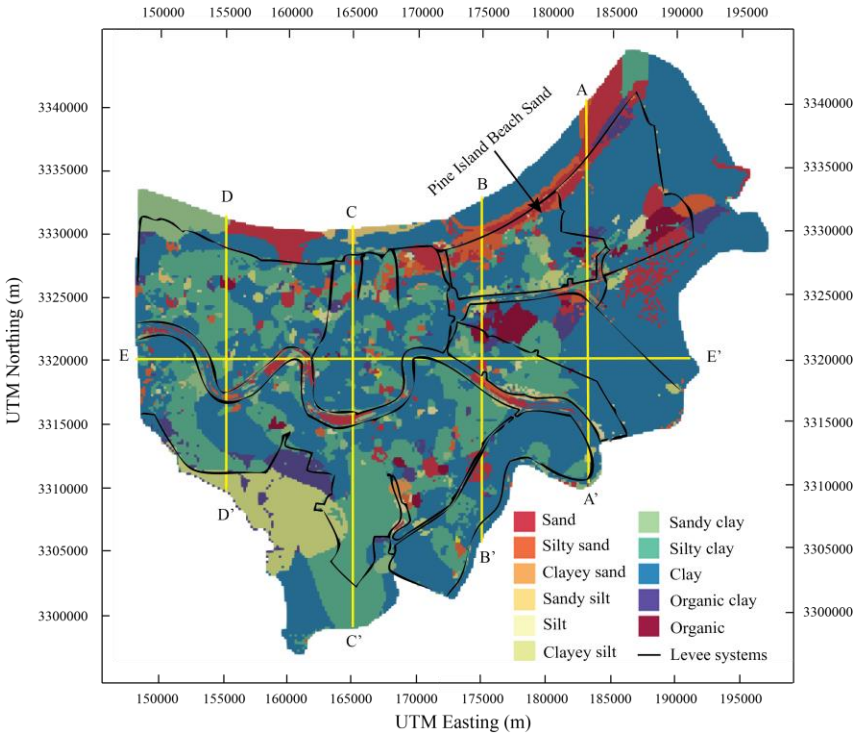

Figure 8. Surficial sediment distribution of the stratigraphy model in New Orleans. Coordinate system is NAD 83 / UTM zone 15N.

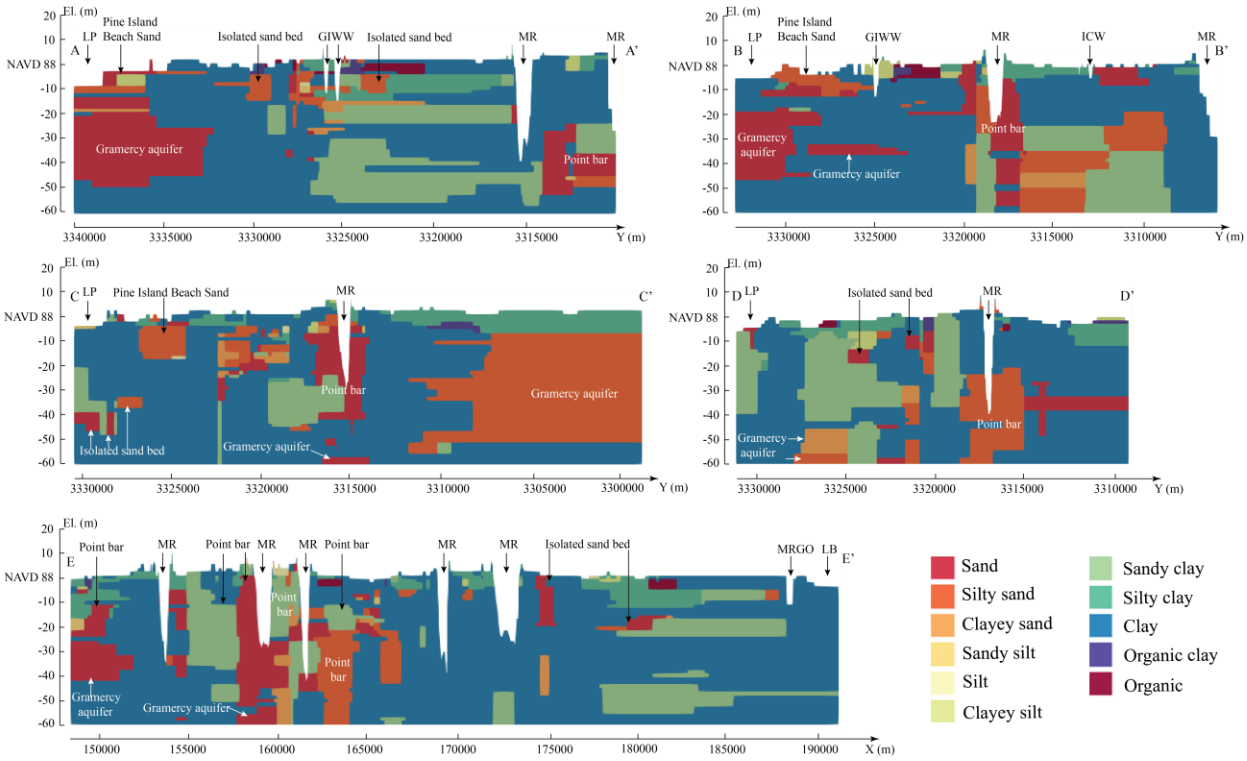

Figure 9. Sediment distributions at the cross sections of Figure 8. LP: Lake Pontchartrain; MR: Mississippi River; LB: Lake Borgne. Coordinate system is NAD 83 / UTM zone 15N. X axis presents UTM Easting. Y axis represents UTM Northing.

In brief, the stratigraphy model developed in this study can reflect the main topographical and geological features that are explored in previous studies. Thus, the stratigraphy can serve as a reliable basis for the groundwater flow model.

5.2. Sensitivity analysis

The significance of parameters in the groundwater flow model was evaluated. Figure 11 shows scaled CSS calculated among 38 control points and four USGS observation wells for 16 parameters. Both figures show the same top 5 sensitive parameters: hydraulic conductivity of sand and clay, specific storage of sand and clay, and the leakance of Mississippi River bed. Scaled CSS values for specific yields of sand, silt, clay and organic are nearly zero, indicating that sediments are fully saturated at the control points and the observation wells. Parameters relating to silt and organic have a relatively low impact on simulated groundwater head because silt and organic are

not extensively distributed around control points and observation wells. Figure 11(b) show that the CSS values for streambed leakance of the IHNC, lakes, Harvey Canal are also relatively low, indicating less sensitive at the USGS observation wells. Therefore, the top five model parameters were selected for model calibration. On the other hand, some parameters, such as the leakance of IHNC and lakes, which have less impact on groundwater head around USGS observation wells could have considerable influence on groundwater head at other control points (Figure 11). Therefore, uncertainties of all parameters are expected to be considered.

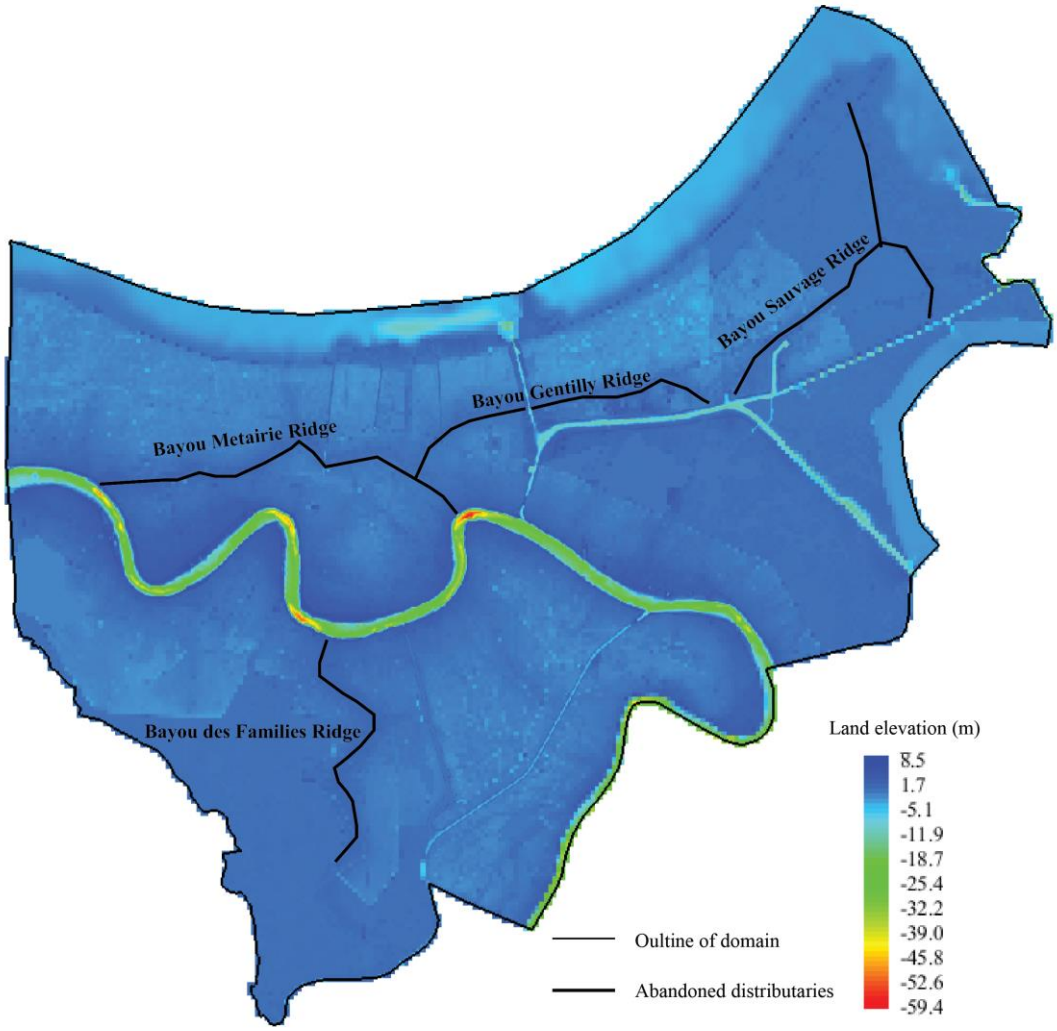

Figure 10. Land surface and stream valley elevation (NAVD 88) in the stratigraphy model. Elevated ridges along the abandoned Mississippi River distributaries are annotated.

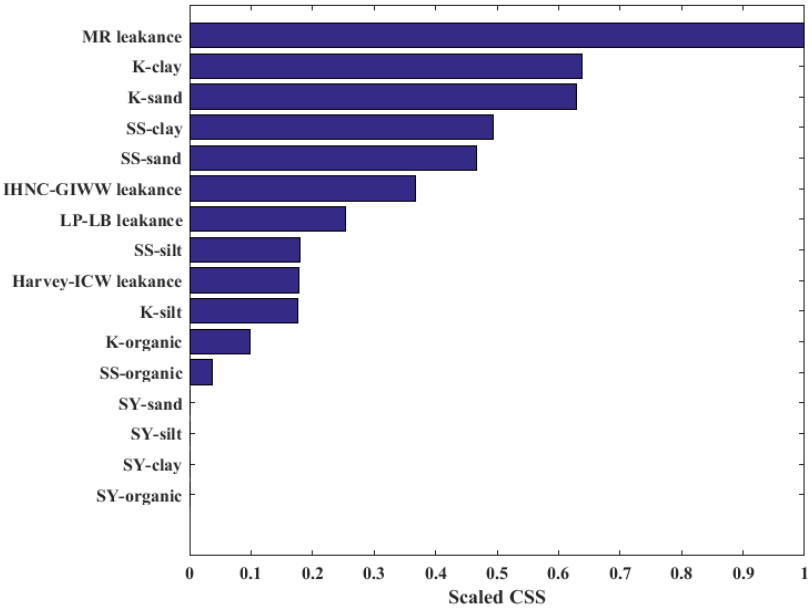

(a)

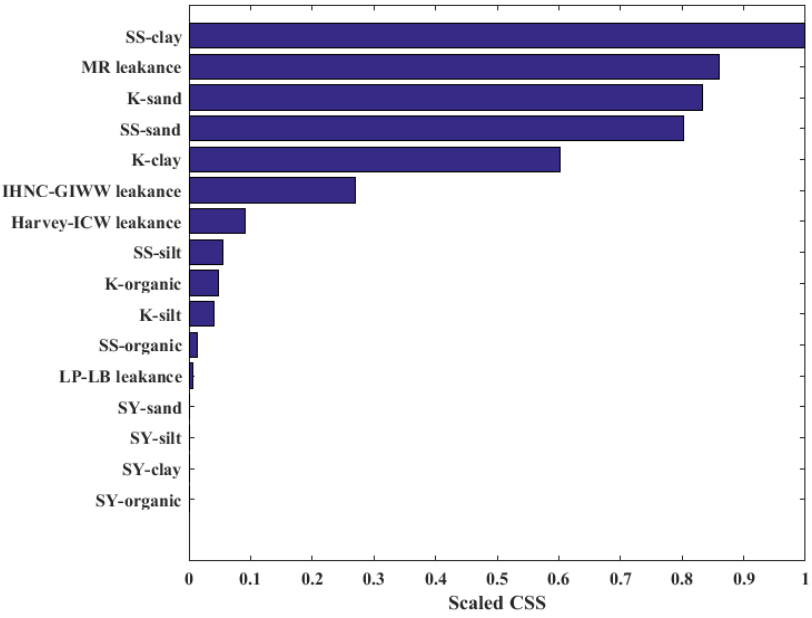

(b)

Figure 11. Scaled CSS of parameters in groundwater flow model among (a) 38 control points and (b) 4 observation wells. MR: Mississippi River. LP: Lake Pontchartrain. LB: Lake Borgne.

5.3. Model calibration and parameter uncertainty

The groundwater model was calibrated with the groundwater level data observed by the USGS. A calibration scenario was performed with the groundwater flow simulation from

10/12/1960 to 10/11/1961 during which observed data is relatively concentrated. In this study, five parameters with largest scaled CSS (more than 0.5) at the USGS observation wells, i.e. the leakance of Mississippi River, hydraulic conductivity of sand and clay, specific storage of sand and clay, were involved in the calibration process. Other parameters were assigned with the median values of respective reference range (shown in Table 3) in the calibration scenario. The calibration was completed by SQP with the RMSE of 0.528 m and the NSE of 0.742, which means that the model has sufficient quality and predictive powers. The parameter values decided after calibration are shown in Table 3. Figure 12 illustrates that most of simulated groundwater heads have less than 1-meter error from the corresponding observed data. As the maximum error of approximately 1 m is not negligible, variability of the model output with regard to parameter uncertainties is important to learn the groundwater level dynamics in the study area.

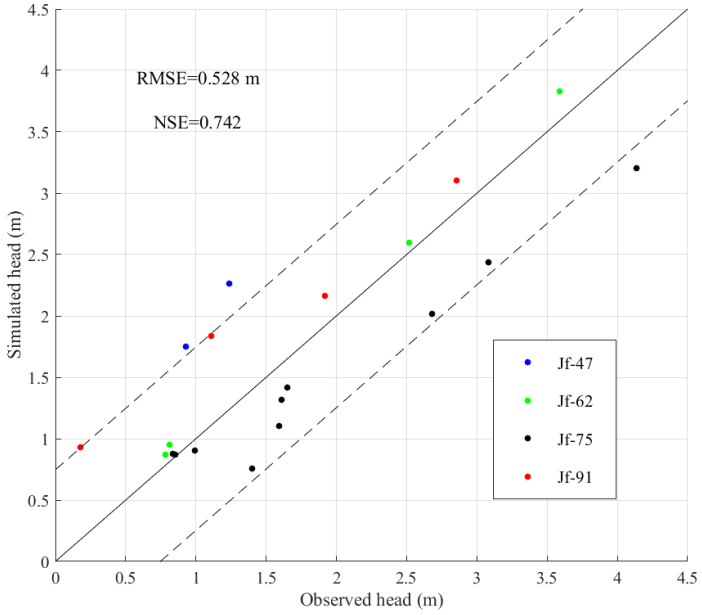

Figure 12. Scatter plot of the observed groundwater heads in USGS observation wells against the groundwater heads simulated by the groundwater flow model with decided parameter values. The dash lines represent one RMSE.

A Monte Carlo simulation was performed with 50 samples to evaluate uncertainties of groundwater head prediction due to the parameter uncertainty. The statistics and assumed

probability density functions of parameters are shown in Table 3. Latin hypercube sampling (LHS) was adopted to sample parameter values. The mean and the variability of groundwater heads from the Monte Carlo simulation in the calibration scenario and the observed groundwater heads at each observation well are shown in Figure 13. Dynamics of the mean simulated head follows the Mississippi River stage, because piezometers in the four observation wells monitored the groundwater levels in point bar sands connecting the river. The shades of one standard deviation of simulated groundwater head in Figure 13 illustrate that simulated groundwater head at the observation wells are not sensitive to the change of parameter values when Mississippi River stage is low. So there is a small variability of simulated groundwater heads at observations if the river is not in flood seasons. Besides, according to the box plots in Figure 13, the simulated groundwater heads at observations don't follow Gaussian distribution, which might result from the nonlinear relationship between simulated groundwater head and parameters in the complicated model.

In addition, the fitness of observed groundwater heads with the variability of simulated heads is displayed in Figure 12 and Figure 13. The simulated heads at the location of Jf-62 fit well with observed data. However, the simulated groundwater heads at the observations in Jf-47 and Jf-91 are overestimated by the model (Figure 13(a), (d)), especially the second observation at Jf-47 and the forth observation at Jf-91 which exceed the variability of the corresponding simulated groundwater head. One reason for this can be pumping's effects on these observation wells. But it is assumed that there is no pumping in the study area because of the lack of data. Besides, the simulated heads at the observations in Jf-75 are underestimated by the model when Mississippi River experience its flood seasons (Figure 13(c)). This can be explained by the heterogeneity of hydrogeological properties. Jf-75 is relatively far away from other concentrated observation wells (Figure 2), so the hydrogeological properties, such as hydraulic conductivity of coarse deposits,

around Jf-75 might be different from that around other wells. But the properties of each sediment group in this study are considered to be homogenous. A majority of observed data matches well with simulated groundwater head or is within its variability. Therefore, simulations with the 50 samples were performed in 2018 for the exploration of groundwater level dynamics and the further assessments of groundwater flooding and levee underseepage.

Table 3. Range, decided value, and probability density function (pdf) of groundwater flow model parameters. MR: Mississippi River. LP: Lake Pontchartrain. LB: Lake Borgne. HC: Harvey Canal. ICW: Intracoastal Waterway.

Parameter	Range	Decided value	pdf
K-sand, m/d	9 to 30 [1,2]	40.4	Gaussian
K-silt, m/d	0.13 to 0.49 [2]	0.31	Uniform
K-clay, m/d	8.6×10^{-5} to 8.6×10^{-3} [3]	0.0001	Gaussian
K-organic, m/d	0.08 to 0.86 [4]	0.47	Uniform
S_s-sand, m^{-1}	1.1×10^{-5} to 1.1×10^{-4} [3]	1.26×10^{-5}	Gaussian
S_s-silt, m^{-1}	9.9×10^{-5} to 9.8×10^{-3} [5]	0.0049	Uniform
S_s-clay, m^{-1}	9.2×10^{-4} to 0.2 [6]	0.01	Gaussian
S_s-organic, m^{-1}	0.014 to 0.052 [4]	0.033	Uniform
S_y-sand	0.27 to 0.33 [7]	0.3	Uniform
S_y-silt	0.05 to 0.15 [8]	0.1	Uniform
S_y-clay	0.02 to 0.08 [7]	0.05	Uniform
S_y-organic	0.13 to 0.48 [5,9]	0.3	Uniform
MR leakance, d^{-1}	8.6×10^{-4} to 0.89 [10,11,12]	0.69	Gaussian
IHNC-GIWW leakance, d^{-1}	8.6×10^{-4} to 0.89 [10,11,12]	0.05 [13]	Uniform
LP-LB leakance, d^{-1}	8.6×10^{-4} to 0.89 [10,11,12]	0.01 [13]	Uniform
HC-ICW leakance, d^{-1}	8.6×10^{-4} to 0.89 [10,11,12]	0.45	Uniform

[1]Duncan et al. (2008)
[2]Dial and Tomaszewski (1988)
[3]Dial and Sumner (1989)
[4]Hogan et al. (2006)
[5]Younger (1993)
[6]Batu (1998);
[7]Heath (1983)
[8]Johnson (1967)
[9]Letts et al. (2000)
[10]Chen and Chen (2003)
[11]Cherkauer and Taylor (1990)
[12]Dysart et al. (1999)
[13]Jafari et al. (2019)
[13]Jafari et al. (2019)

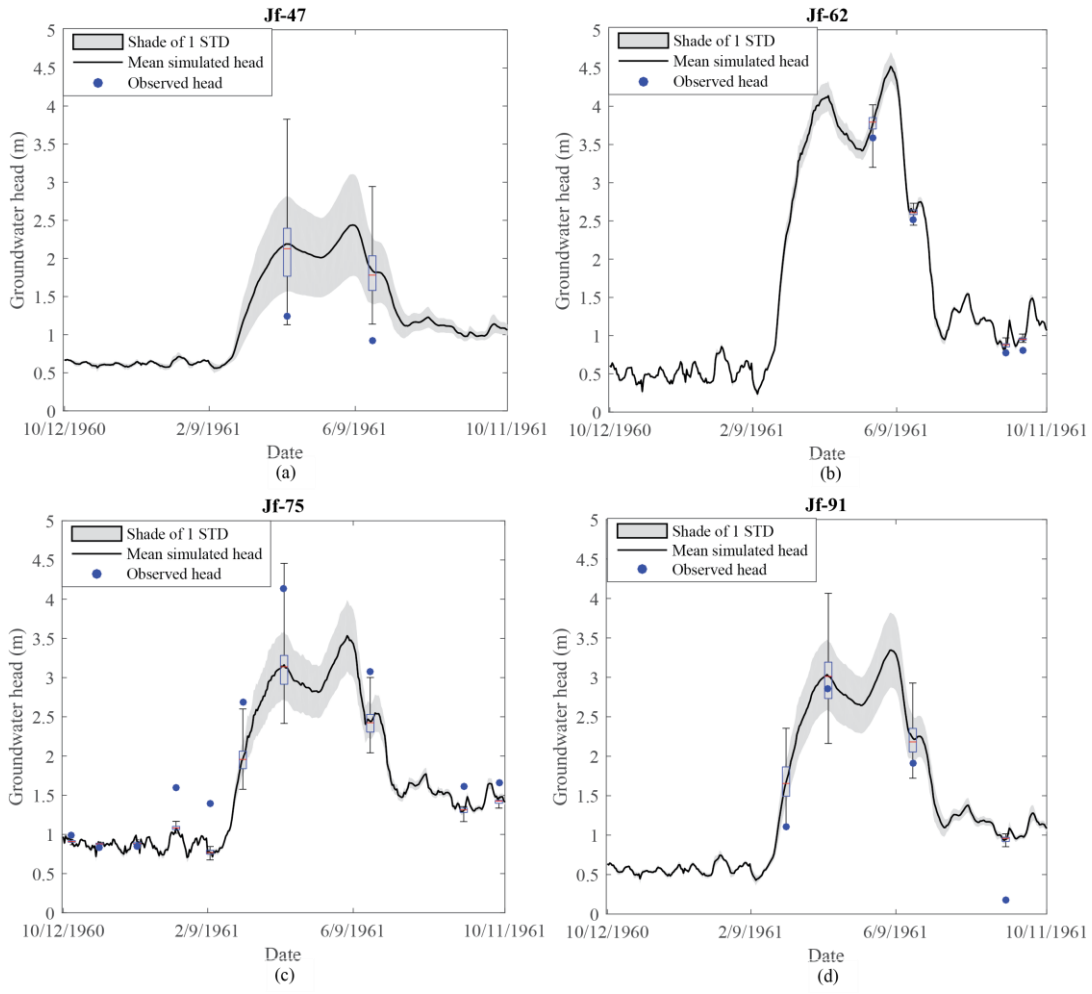

Figure 13. Simulated groundwater head and its uncertainty at each observation well: (a) Jf-47, (b) Jf-62, (c) Jf-75, and (d) Jf-91 in the calibration scenario. Box plots display the variabilities of simulated heads at observations based on minimum, first quantile, median, third quartile, and maximum. Mean and standard deviation of the simulated groundwater head at each observation well are shown as black line and grey shade, respectively.

5.4. Groundwater level dynamics of 2018

Groundwater level distribution that was simulated in 2018 with 50 samples was used to learn interactions between groundwater and surface water in New Orleans. Hydrographs of each surface water in 2018 is shown in Figure 7. Figure 14 displays mean simulated groundwater level in New Orleans at 5 representative days during a flood season of Mississippi River in 2018. Mississippi River stage in New Orleans varies from 0.5 m to 5.7 m during the flood season while water stages in other surface water only range within 1.0 meter of mean sea level as there was no

hurricane or storm event. The five maps in Figure 14 illustrate high groundwater level in the east and central areas and along Mississippi River, which is the result of relatively high Mississippi River water stage. High river water can propagate into coarse sands and silt and result in high groundwater level in those pockets along Mississippi River. There is 0.89 m to 1.59 m difference between the river stage and the groundwater levels in those pockets when the river is at a peak stage (Figure 14(c)). Also, groundwater level adjacent to Mississippi River can remain higher than river stage after the peak river stage due to relatively slow response of groundwater to river dynamics, which is apparent for a river reach between IHNC Lock (01340) and Algiers Lock (01380) (locations of locks are shown in Figure 2). The water stage on June 30th in the river reach was between 1.28 m and 1.30m while the groundwater level adjacent to the east bank of the river reach ranged from 1.37 m to 2.35 m (Figure 14(e)).

Besides, Figure 14 shows relatively low groundwater level along Harvey Canal and ICW, suggesting their strong hydraulic connections with underlying coarse sediments. Harvey Canal and ICW may act as drains of groundwater when their water stages are low. Simulated groundwater levels in the areas near the IHNC, GIWW, and the lakes are close to the surface water stages, which indicates that groundwater levels in these areas would be hardly influenced by Mississippi River. The groundwater head variation along the GIWW indicates hydraulic connections to underlying coarse sediments and potential hydraulic pressure propagation underneath the Lake Borgne Surge Barrier near the confluence of the GIWW and the MRGO. Moreover, groundwater level in the Pine Island Beach sand varies from 0.03 m to 0.24 m when water stages of IHNC and Lake Pontchartrain fluctuated from -0.08 m to 0.31 m (Figure 14), which suggests that groundwater level in the beach sand directly responds to water stages of the IHNC and Lake Pontchartrain due to strong hydraulic connections.

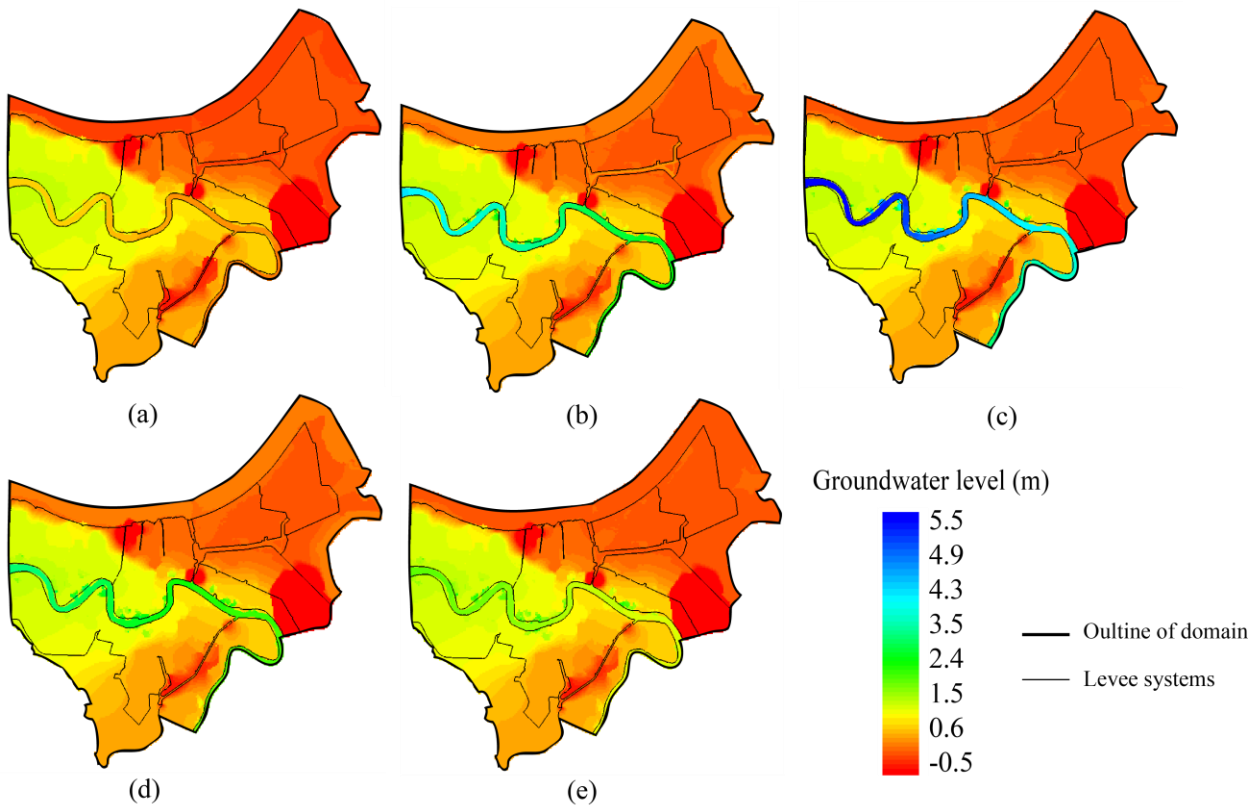

Figure 14. Mean groundwater level in the study area among 50 simulations on (a) January 18th, (b) February 28th, (c) March 21st, (d) May 27th, and (e) June 30th, respectively, in 2018.

5.5. Seepage in urban areas

High groundwater head relative to land surface might indicate high pore water pressures and potential groundwater flooding. Groundwater head above land surface in New Orleans with low and high Mississippi River stage in 2018 is mapped using the mean of simulated groundwater head from Monte Carlo simulation. The maps are shown in Figure 15. Apparent difference of groundwater head above surface between Figure 15(a) and (b) occurs only along Mississippi River, because stages of other surface water are stable in 2018 (Figure 7). Figure 15(a) shows that groundwater head along Mississippi River is lower than land surface, which means that areas along the river are not exposed to groundwater flooding when Mississippi River stages are at base levels. Groundwater head is still below surface in the areas adjacent to parts of the river banks (shown in

Figure 15(b)) during the flood season of the river in 2018. These areas either have natural levees with high elevations or have no aquifers connecting with surface water. Figure 15(b) also illustrates that other areas adjacent to the river banks have groundwater head 0.5 to 2 meters higher than land surface when the river is at peak stage in 2018, which results from strong connections between Mississippi River and buried point bar sands. Besides, areas along the Bayou Metairie-Gentilly ridges and the Bayou des Families ridge with groundwater head below land surface are shown in Figure 15. Both of the ridges are abandoned Mississippi River distributaries with elevated natural levees, which is illustrated in Figure 10. Therefore, areas along these ridges are not exposed to the high groundwater level above land surface. Moreover, according to Figure 15, groundwater level in the undeveloped areas close to MRGO, GIWW, and Lake Borgne is below or no more than 0.5 meter above land surface. Groundwater level above land surface generally varies from 0.5 to 4 meters in the urban areas away from Mississippi River and its distributaries. And the regions north to the Bayou Metairie-Gentilly ridge usually have higher groundwater head relative to land surface compared to those south to the ridge, partially because of the historical groundwater-drain induced land subsidence along the southern shore of Lake Pontchartrain (ILIT, 2006). In particular, groundwater level in the areas east to the northern part of IHNC is 2 to 4 meters above land surface, which suggests high potentials of groundwater flooding. However, the high groundwater head in aquifers above surface cannot directly cause severe groundwater flooding.

Groundwater seepage rate is determined by the groundwater level in top stratum and the permeability of surficial sediments. Seepage rate was calculated in 50 simulations using equation (11) at each surface cell of the groundwater flow model, and the mean seepage depth among 50 simulations in urban areas of New Orleans was mapped. Figure 16(a) and (b) displays mean seepage depth in urban areas of New Orleans on the days with low and high stage of Mississippi

River in 2018, respectively. The main difference between these two maps lies in the areas along Mississippi River: no seepage occurs with low river stage while it potentially occurs parts of the river with the depth up to 4.3 mm when the river stage is at the peak level in 2018 (Figure 16(b)). Relatively large seepage depth ranging from 2.5 to 4.3 mm occurs at a few locations adjacent to high-staged Mississippi River (Figure 16(b)), which results from high water table relative to surface in thin silty and sandy top stratum. Except for these locations, seepage depth along Mississippi River is no more than 0.1 mm when the river is at high stage (Figure 16(b)), though the groundwater head in buried point bar sands is above surface in the areas along many parts of the river (Figure 16(b)). The areas with relatively small seepage depth (less than 0.1 mm) along Mississippi River are covered by clay blankets (Figure 8) with low permeability (Table 3). Groundwater level in the top of the blankets are hardly impacted by the groundwater head in underlying aquifers and the river stage during a seasonal flood of the river, which results in a majority of areas along the river with groundwater level below land surface. Although groundwater level in top stratum is higher than land surface in some areas covered by clay blankets along the river, the clay blankets are much less permeable than silty or sandy sediments (Table 3). Therefore, limited or no seepage occurs in the areas covered by clay blankets along Mississippi River with a peak stage.

In addition, seepage depth in urban areas away from the river shown in Figure 16(a) and (b) is similar because of the limited influence of Mississippi River and the relatively stable stages of other surface water during 2018. Wide-spread areas (Gentilly to Little Woods) with relatively large seepage rate (up to 5 mm per day) adjacent to IHNC, London Ave Canal, and parts of the shore of Lake Pontchartrain in 2018 are illustrated in Figure 16. The seepage is caused by the high water table in the Pine Island Beach sand that hydraulically connects to IHNC and Lake

Pontchartrain. With the similar cause, considerable local seepage occurs from sand beds near surface in the areas near the 17th Street Canal, Harvey Canal, and ICW (Figure 16). The seepage depth in these areas varies from 1.5 to 4 mm per day. Furthermore, Figure 16 displays seepage rate ranging from 2 to 3 mm per day in locations of the Lower Ninth Ward. The seepage comes from saturated surficial organic matters. Mean seepage depth of about 4.5 mm per day also occurs discretely at some locations away from Mississippi River (Figure 16).

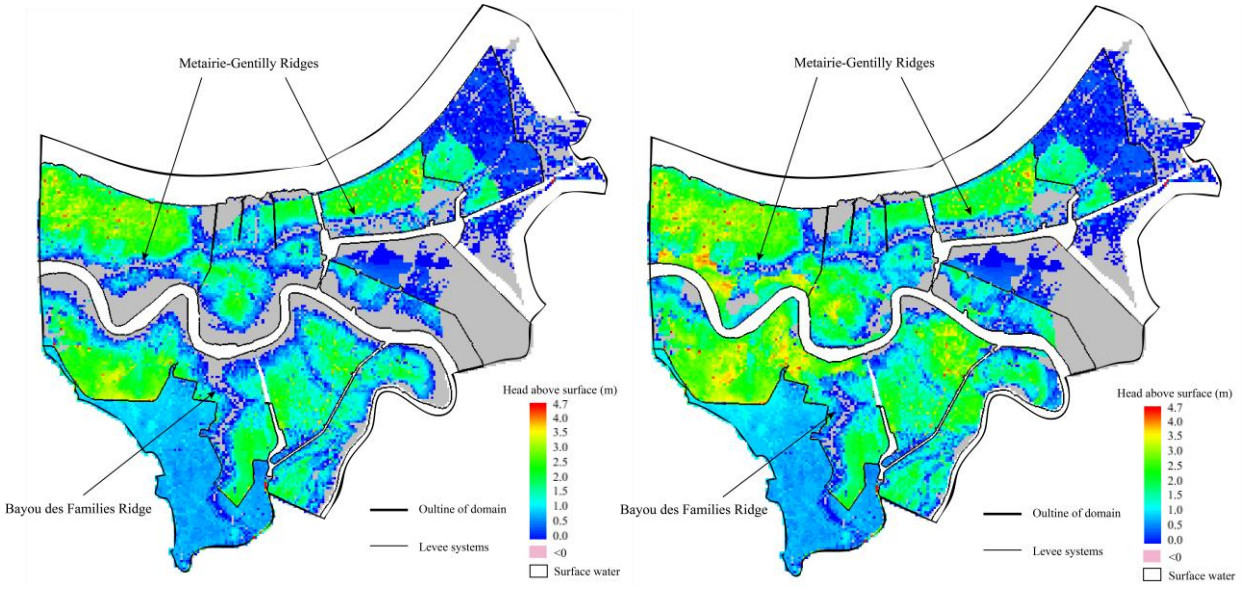

(a) (b)

Figure 15. Mean groundwater head above land surface among 50 simulations on (a) January 18th (low Mississippi River stage) and (b) March 21st (high Mississippi River stage) in 2018. Grey areas are places where groundwater head is below land surface. White areas are surface water.

Moreover, Figure 17 displays the mean of daily seepage depth during a flood season of Mississippi River (from January 27th to July 3rd) in 2018. The averaged daily seepage depth along Mississippi River during its flood season is less than 1.5 mm. The standard deviation of the daily seepage depth varies from 0.5 to 1.8 mm in the areas covered by thin silty and sandy top stratum along Mississippi River. This suggests that seepage in these areas is highly impacted by the river stage. But the standard deviation is very small with the maximum of 2.5×10^{-2} mm in other areas

that are adjacent to surface water and exposed to considerable seepage rate, because of the relatively stable water stages in lakes, canals, and waterways in 2018.

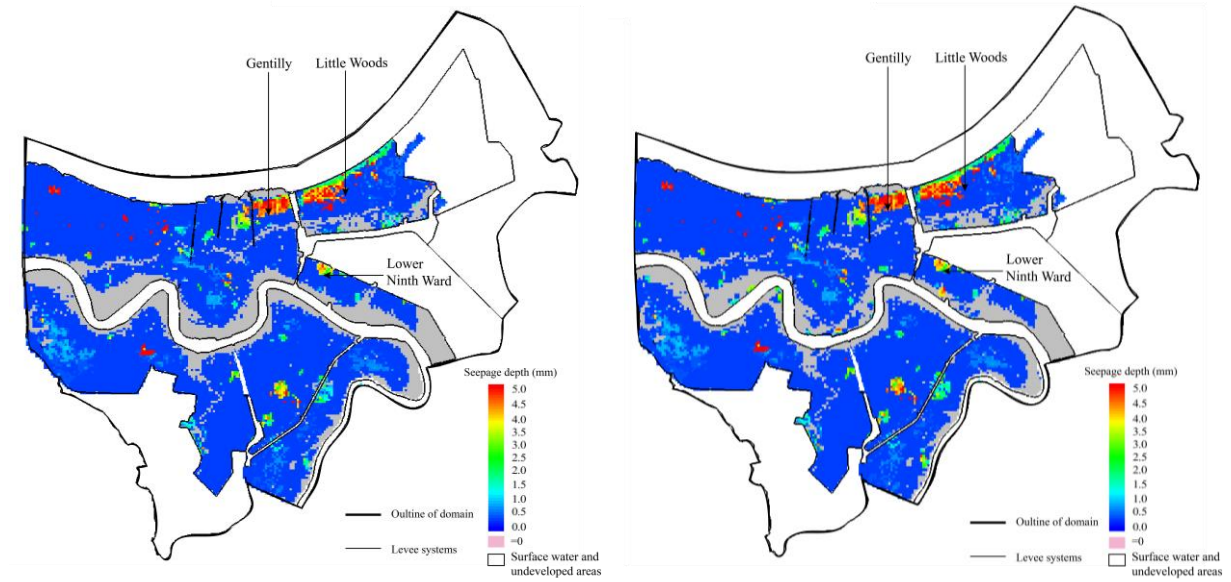

(a) (b)

Figure 16. Mean seepage depth in urban areas of New Orleans among 50 simulations on (a) January 18th (low Mississippi River stage) and (b) March 21st (high Mississippi River stage) in 2018. White areas are undeveloped areas and surface water areas.

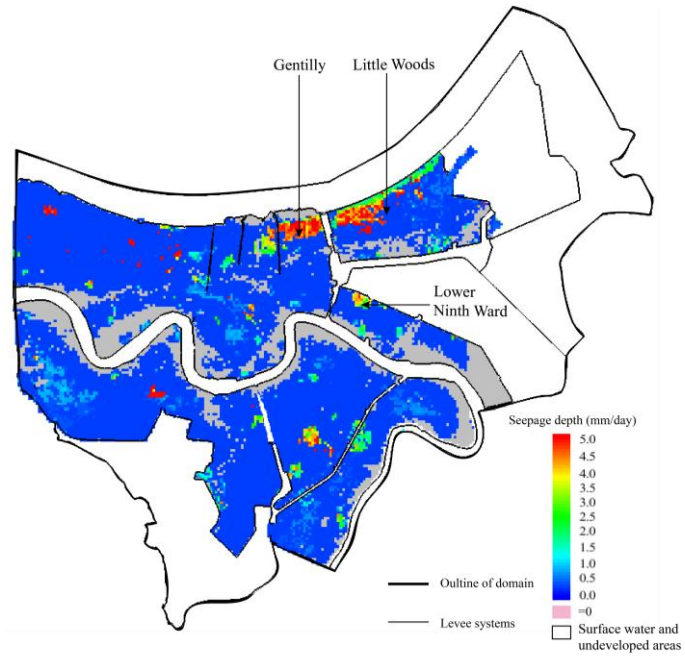

Figure 17. Averaged seepage depth in urban areas during a flooding season (from January 18th to July 3rd) of Mississippi River. White areas are undeveloped areas and surface water areas.

In summary, the mean seepage depth with range from 1.5 to 5 mm per day are concentrated in the areas adjacent to London Ave Canal, IHNC, parts of Lake Pontchartrain, Harvey Canal and ICW in 2018. These areas are subject to relatively severe and long-lasting groundwater flooding. Nevertheless, the majority of the vicinity area of the Mississippi River appears to have a negligible groundwater flooding issue during a flood season of the river in 2018.

5.6. Factor of safety

FS against uplift is used to reflect the risks of sand boils and the severity of underseepage along levees in New Orleans. The thickness of top stratum was transformed using equation (14). The map of transformed top stratum thickness is shown in Figure 18. A substratum was determined as the first coarse-sediment layer that has the thickness greater than 3 meters. FS at each location was computed by equation (13) using the transformed thickness and the groundwater head from Monte Carlo simulation. The map of mean FS against uplift in New Orleans when the Mississippi river stage is high in 2018 (on March 21st) is shown in Figure 19(a). In this study, FS against uplift along levees is of interest which is generally at least to be 1.0 to get rid of sand boils (USACE, 1992). Low FS along levees resulting from excessive pore water pressures in pervious stratum can indicate strong underseepage and potential sand boils which might impact the stability of levee foundations (Stark et al., 2014). But low FS cannot directly indicate the occurrence of sand boils or levee failures. The areas along most parts of Mississippi River levees have high FS (greater than 1.0). The reason for this phenomenon is that thick blankets usually exist along the Mississippi River banks (Figure 18) because of the presence of elevated natural levees consisting of fine-grained sediments, and thus, vertical hydraulic gradient (i_v) is low. But a few locations with FS less than 1.0 are found adjacent to Mississippi River levee in New Orleans, because point bar sands at those locations are shallowly buried in natural levees (Figure 18) and have high groundwater

head when the river experiences its flood seasons (Figure 15 (b)). In addition, Figure 19(a) illustrates the areas with low FS away from Mississippi River, as blankets in these areas are not as thick as that along the river, such as the areas near the southern part of 17th Street Canal levee. Areas along levees of London Ave Canal, IHNC (north to GIWW), and Lake Pontchartrain also have FS less than 1.0, which results from high pore water pressures in the Pine Island Beach sand. Similarly, low FS along levees of Harvey Canal and ICW is caused by high water table in adjacent sand beds. FS along some parts of levees of GIWW and the surge barrier in Lower Ninth Ward is also small (Figure 19(a)). Moreover, Figure 19(a) suggests some risky locations at the bathymetries of GIWW, Lake Pontchartrain, and Harvey Canal. "Sand boils" might potentially occur at these locations, especially in Lake Pontchartrain, which results from occasional high groundwater head in coarse grains at the bathymetries that exceeds the dynamic surface water stages.

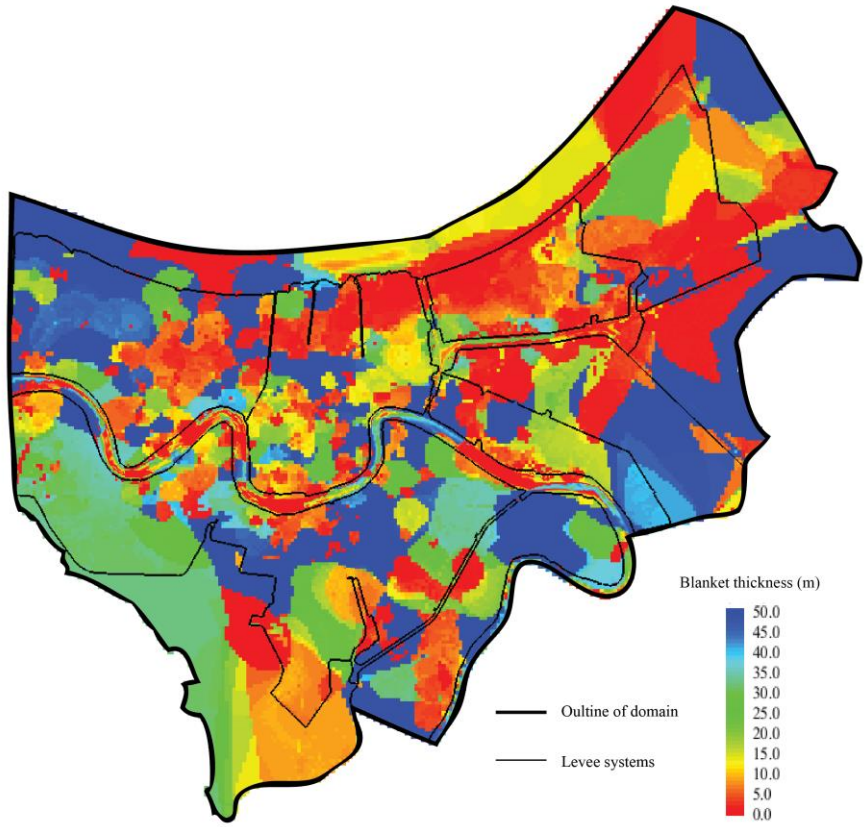

Figure 18. Transformed blanket thickness in the study area.

The uncertainties of parameters in the groundwater flow model result in large variabilities of FS along levees in New Orleans. Probability of having FS less than 1.0 at each location with high Mississippi River stage (on March 21st) in 2018 was calculated based on results of 50 simulations (shown in Figure 19(b)). The probability is interpreted by the percentage of cases with FS less than 1.0 out of the 50 simulations. The areas with high probability that is over 80 percent usually coincide with the areas where the mean FS is less than 1.0 in Figure 19(a), including the levees of the northern IHNC, Lake Pontchartrain, GIWW, the southern 17th Street Canal, London Ave Canal, Harvey Canal, ICW, and the surge barrier in Lower Ninth Ward. However, some locations with the chances of low FS (less than 1.0) are not reflected in Figure 19(a). Some locations adjacent to the east bank of upstream Mississippi River have considerable probability of low FS varying from 4 to 84 percent. These locations are underlain by shallow buried point bar sands connecting to Mississippi River.

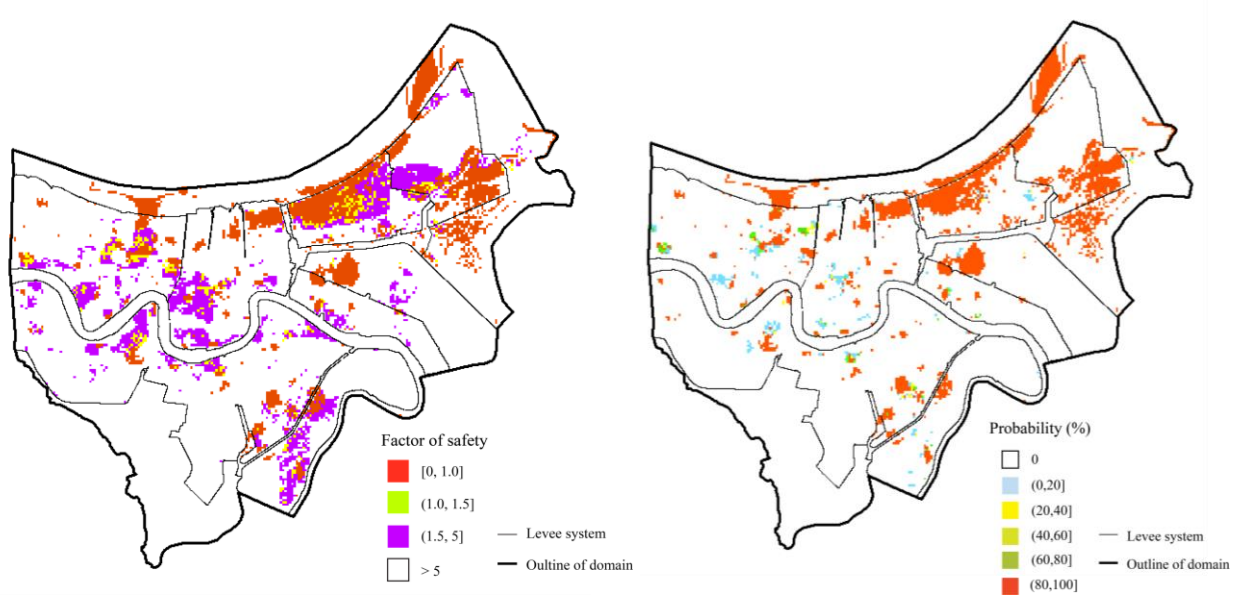

(a) (b)

Figure 19. FS against uplift on March 21st (High Mississippi River stage), 2018, and its uncertainty in the study area, (a) map of mean FS, and (b) probability of having FS less than 1.0.

5.7. Discussions

In this section, the impacts of hydrogeology on groundwater flooding in New Orleans area are pointed out, and the features of groundwater flooding in the city are summarized. Besides, the results of levee underseepage assessment are compared with previous studies. Moreover, some future work that can improve the reliability of the groundwater flow model and the assessments is described.

5.7.1. Groundwater flooding

This study can reflected the relationship between groundwater flooding and hydrogeology in New Orleans. Groundwater flooding in New Orleans is triggered by the high water table in shallow aquifers that receive strong recharge from surface water, which corresponds to the second type of groundwater flooding (Macdonald et al., 2008). According to Figure 15, there are 40% to 54.7% of the urban areas (depending on surface water stages) where groundwater level is over 1 meter higher than land surface. But only 4.5% to 5.3% of the urban areas might be subject to considerable groundwater flooding, due to the relatively severe seepage rate (> 1.5 mm per day) which is shown in Figure 16. Therefore, high groundwater head in aquifers may not result in severe groundwater flooding. Groundwater flooding depends on both of water table in surficial sediments and their permeability. Relatively severe groundwater flooding usually comes from well recharged surficial silty and sandy sediments with high water table, such as the Pine Island Beach sand along the shore of Lake Pontchartrain, because these sediments are relatively permeable and are able to cause notable seepage. In contrast, the groundwater flooding issue might not be a concern in an area that is covered by a less permeable blanket (clay strata) though the area is adjacent to high-staged surface water or underlain by aquifers with high groundwater head.

The spatial distribution of groundwater flooding in New Orleans is explored in this study. Unlike the flooding caused by levee overtopping or elevated tides and surges which is concentrated along rivers and coastlines, groundwater flooding can occur discretely in New Orleans depending on local hydrogeological properties (Figure 17). Moreover, due to the low land elevation, groundwater flooding may occur in the areas adjacent to IHNC, Lake Pontchartrain, London Ave Canal, Harvey Canal, and ICW all year around (Figure 17), though the stages of these surface water are at base level in 2018. The prolonged flooding has large impact on stability of infrastructures, such as roads, because groundwater flooding usually comes with uplift forces (Morris et al., 2018). On the other hand, groundwater flooding along Mississippi River in New Orleans is seasonal and is highly related with the dynamics of the river stage (Figure 16). And the assessment of groundwater flooding suggests that the majority of the vicinity area along the river are not exposed to the emergence of groundwater on land surface. But groundwater flooding might be invisible on surface as it can occur underground, for instance, inundations of basements (Macdonald et al., 2008).

Groundwater flooding discussed in New Orleans can be an indication for that in other coastal areas. Many coastal cities, such as Lagos and Surat, have similar hydrological conditions to the study area, including low-lying urban areas covered by fine grains, rivers with high stages during flood seasons passing through the cities, drainage channels developed for storm events, etc. (Adelekan, 2010; Bhat et al., 2013). Therefore, groundwater flooding in these cities might occur at the low-lying locations if there are shallow aquifers hydraulically connecting with surface water when the water stages rise to critical levels. However, the occurrence of groundwater flooding cannot be asserted without a full understanding of local hydrogeological settings.

5.7.2. Underseepage in New Orleans

The areas with underseepage issues identified in this study can be correlated with levee breach mechanisms during Hurricane Katina. Although underseepage analysis was performed in 2018 during which water stages of lakes and canals are low and stable, the results can still reflect potential levee failure reasons in New Orleans during hurricanes or storm events. As mentioned in section 1.2, previous research focused on the major levee breaches during Katrina at the 17th Street Canal, London Ave Canal, and IHNC, because these levee breaches occurred before overtopping. In this study, the underseepage-based FS analysis indicates that the FS against uplift is low (less than 1.0) with over 80% chance along parts of London Ave Canal levee, while the areas along the northern part of the 17th Street Canal levee and the southern part of IHNC levee (in the Lower Ninth Ward) have low probability of FS against uplift < 1.0 (Figure 19). This means that levee underseepage can play a considerable role in levee instability along London Ave Canal, but the levee safety issues along the northern 17th Street Canal and the southern IHNC, at least when water stages of lakes and canals are low, might not be attributed to underseepage. This finding is supported by the studies of IPET (2006) and Dunbar and Britsch (2008) about levee failure mechanisms during Katrina. The 17th Canal breach was likely due to weak lacustrine soils with rich organic matter. The IHNC breaches were likely caused by overtopping that created a scour trench and reduced levee's stability (Dunbar and Britsch, 2008). Besides, strong underseepage are identified by the FS analysis along the northern part of the IHNC levee and some locations along the GIWW levee (Figure 19). These parts of levees were damaged during Katrina, which is shown in the map of levee damage sites produced by IPET (2006). But the mechanisms were not fully investigated. This study suggests that the strong underseepage can be one of the potential contributors to these damages.

In addition to the levees mentioned above, potential sand boils introduced by underseepage are indicated by the FS analysis along some other parts of the flood protection systems in New Orleans. These risky areas with the FS less than 1.0 are concentrated along parts of Lake Pontchartrain levee, the southern part of the 17th Street Canal levee, parts of Harvey Canal and ICW levees. And uncertainty analysis indicates that these areas have over 80 percent of probability to have the low FS (Figure 19(b)). In contrast, FS along most parts of Mississippi River levee is high due to the high and thick natural levees consisting of fine grains, except for a few discrete locations underlain by elevated point bar sands (Figure 19(a)). Some areas adjacent to the river banks also have highly uncertain FS (Figure 19(b)). These areas are also underlain by the point bar sands that are buried in shallow depths (Figure 18). Therefore, the Mississippi River levee in New Orleans is not completely exempted from strong underseepage, though no sand boil along the levee was reported before. In brief, apart from the levees that have experienced failures, some other parts of flood protection system in New Orleans are also subject to strong underseepage that might impact levee foundations.

5.7.3. Perspective research

The groundwater flow model developed in this study can be improved with more observations. The model was calibrated with limited observed groundwater head data which comes from four local observation wells which are distributed in a concentrated manner. The limited data results in that a limited number of parameters in the model were involved in the calibration. Therefore, the accuracy of the model output and the reliability of assessments can be enhanced if the observed data widely distributed in the study area can be collected in the future.

The methods to compute groundwater flooding are not unique. Korkmaz et al. (2009) obtained the volume of water joining the surface runoff by computing the hydrological water

balance at surface cells in a surface water model. The surface water model can simulate runoff caused by groundwater flooding and predict inundated areas. In this study, the severity of groundwater flooding was reflected by seepage rate that was calculated by Darcy's law under the condition that the shallow groundwater head distribution and the stratigraphy were obtained. This method was proved to produce groundwater flooding rates similar to measured values in the UK (Morris et al., 2018). Further research might focus on the combination of the groundwater flow model and a hydraulic model. After the volume of groundwater emerged on land surface is computed, the hydraulic model can simulate the runoff of the emerged water on land surface with drainage networks, which can make groundwater flooding extent mapped with better accuracy.

The groundwater flow simulations in 2018 were performed with relatively low surface water stage (except for Mississippi River) in this study and results about the severity of groundwater flooding and levee underseepage might be optimistic. However, areas with notable underseepage and considerable groundwater flooding still exist adjacent to surface water, especially IHNC and Lake Pontchartrain. Therefore, if there is a hurricane or storm event during which lake stages rise and then canals and waterways are back filled, risks of sand boils along the levees can be even higher and groundwater flooding in urban areas might be more severe. The analyses of groundwater flooding and levee underseepage in the scenarios with hurricanes or storm events can be future work.

6. Summary and Conclusions

This study focused on groundwater flow model development, groundwater flooding, and levee underseepage in New Orleans. In the model development process, the MINN interpolation method was developed to construct a stratigraphy model. Based on the stratigraphy, the groundwater flow model was designed using MODFLOW-USG. CSS was computed to rank the significance of parameters in the model. Then the model was calibrated with observed groundwater head data by SQP. 50 samples were generated to conduct Monte Carlo simulation. Uncertainties of simulated groundwater heads in the calibration scenario at observation wells were quantified. With these samples, simulations were performed in the year of 2018 to evaluate groundwater level dynamics, groundwater flooding and levee underseepage in New Orleans under normal climatic conditions. Groundwater flooding was quantified by Darcy's law. Mechanisms and features of groundwater flooding in New Orleans were explored. Severity of levee underseepage and potentials of sand boils were assessed by the FS analysis. Some findings from the model development and analyses on groundwater flooding and levee underseepage in New Orleans can be concluded:

1) The stratigraphy model showed that New Orleans is rich in clay in upper 60 meters; 74% of sediments in shallow New Orleans are fine grains (clay and silty clay); The Pine Island beach sand along the shore of Lake Pontchartrain is the most pronounced shallow sand that connects to the lake and IHNC; Point bars consisting of various sediments directly contact Mississippi River; Sandy sediments near surface have connections with ICW and GIWW;
2) Groundwater flow simulations suggests that groundwater level in the areas near IHNC, GIWW, and lakes is hardly influenced by the Mississippi River stage; Harvey Canal and ICW might act as drains of groundwater when their water stages are low;

3) By simulating groundwater flow in 2018, the study found that 40% of New Orleans metropolitan area may have groundwater head 1.0 m above ground surface all year round; Residential areas around IHNC in the vicinity of Lake Pontchartrain are the most concerned about groundwater flooding that comes from Pine Island Beach sand; Groundwater flooding is unlikely to occur in the vicinity areas of Mississippi River, except for those areas covered by shallow sands;
4) High groundwater head may not directly cause severe groundwater flooding in New Orleans; Relatively severe groundwater flooding comes from well recharged surficial coarse sediments with high water table; But groundwater flooding might be negligible in the area that is covered by a blanket with low permeability though the area is adjacent to high-staged surface water or underlain by aquifers with high groundwater head;
5) Factor of safety analysis suggests that in addition to the London Ave Canal levee which failed during Katrina, parts of the levees of Lake Pontchartrain, the northern IHNC, GIWW, the southern 17th Street Canal, Harvey Canal, and ICW are also subject to strong levee underseepage even under normal climatic conditions; A few locations along the Mississippi River levee may be also vulnerable to sand boils though areas along the river are protected by elevated natural levees.

This study revealed the impacts of hydrogeology on groundwater flooding, and provided a picture of potential underseepage-induced hazards, such as sand boils, in New Orleans. The analyses of groundwater flooding and factor of safety against uplift in New Orleans can be used as a reference by city planners to manage and maintain infrastructures. Also, the results in this study can provide an indication of these hazards in other coastal cities with similar hydrogeological conditions around the world.

References

Adams, B. et al., 2010. An early warning system for groundwater flooding in the Chalk. Quarterly Journal of Engineering Geology and Hydrogeology, 43(2): 185-193. https://doi.org/10.1144/1470-9236/09-026

Adelekan, I.O., 2010. Vulnerability of poor urban coastal communities to flooding in Lagos, Nigeria. Environment & Urbanization, 22(2): 433-450. https://doi.org/10.1177/0956247810380141

Ahmed, A.A., Bazaraa, A.S., 2009. Three-dimensional analysis of seepage below and around hydraulic structures. Journal of Hydrologic Engineering, 14(3): 243-247.

Arsenault, R., Poulin, A., Côté, P., Brissette, F., 2013. Comparison of stochastic optimization algorithms in hydrological model calibration. Journal of Hydrologic Engineering, 19(7): 1374-1384.

Ascott, M.J., Marchant, B.P., Macdonald, D., McKenzie, A.A., Bloomfield, J.P., 2017. Improved understanding of spatio-temporal controls on regional scale groundwater flooding using hydrograph analysis and impulse response functions. Hydrological processes, 31(25): 4586-4599. https://doi.org/10.1002/hyp.11380

Ayyub, B.M., Lai, K.-L., 1989. Structural reliability assessment using latin hypercube sampling, Structural Safety and Reliability. ASCE, pp. 1177-1184.

Baalousha, H. et al., 2008. Fundamentals of groundwater modelling, in: Groundwater: Modelling, Management, and Contamination., Konig, L.F., Weiss, J.L. (Eds). Nova Science, UK, pp 113-130.

Bard, Y., 1974. Nonlinear Parameter Estimation. Academic Press, New York.

Batu, V., 1998. Aquifer Hydraulics: A Comprehensive Guide to Hydrogeologic Data Analysis. John Wiley and Sons, New York.

Bekesi, G., McConchie, J., 1999. Groundwater recharge modelling using the Monte Carlo technique, Manawatu region, New Zealand. Journal of Hydrology, 224: 137-148.

Bhat, G.K., Karanth, A., Dashora, L., Rajasekar, U., 2013. Addressing flooding in the city of Surat beyond its boundaries. Environment & Urbanization, 25(2): 429-441. https://doi.org/10.1177/0956247813495002

Boggs, P.T., Tolle, J.W., 1995. Sequential quadratic programming. Acta numerica, 4: 1-51. https://doi.org/10.1017/S0962492900002518

Boggs, P.T., Tolle, J.W., 2000. Sequential quadratic programming for large-scale nonlinear optimization. Journal of Computational and Applied Mathematics, 124(1-2): 123-137. https://doi.org/10.1016/S0377-0427(00)00429-5

Calcagno, P., Chilès, J.-P., Courrioux, G., Guillen, A., 2008. Geological modelling from field data and geological knowledge: Part I. Modelling method coupling 3D potential-field interpolation and geological rules. Physics of the Earth and Planetary Interiors, 171(1-4): 147-157.

Chen, M., Izady, A., Abdalla, O.A., Amerjeed, M., 2018. A surrogate-based sensitivity quantification and Bayesian inversion of a regional groundwater flow model. Journal of Hydrology, 557: 826-837.

Chen, Q., Zhang, L., 2006. Three-dimensional analysis of water infiltration into the Gouhou rockfill dam using saturated unsaturated seepage theory. Canadian Geotechnical Journal, 43(5): 449-461.

Chen, X., Chen, X., 2003. Sensitivity analysis and determination of streambed leakance and aquifer hydraulic properties. Journal of Hydrology, 284(1-4), 270-284. https://doi.org/10.1016/j.jhydrol.2003.08.004

Cheng, H.-P., Winters, K.D., England, S.M., Pickett, R.E., 2014. Seepage-based factor of safety analysis using 3D groundwater simulation results. ERDC/CHL CHETNXI-2. U.S. Army Engineer Research and Development Center, Vicksburg, MS..

Chin, W.W., Marcolin, B.L., Newsted, P.R., 2003. A partial least squares latent variable modeling approach for measuring interaction effects: Results from a Monte Carlo simulation study and an electronic-mail emotion/adoption study. Information Systems Research, 14(2): 189-217.

Cherkauer, D. S., Taylor, R. W., 1990. The spatially continuous determination of groundwater flow to surface water bodies: application to the connecting channels between Lakes Huron and Erie. Journal of Hydrology, 114(3-4), 349-369. https://doi.org/10.1016/0022-1694(90)90065-6

Cobos-Roa, D., Bea, R., 2008. Three-dimensional seepage effects at three New Orleans levee breaches during Hurricane Katrina. Electronic Journal of Geotechnical Engineering, 13: 1-26.

Dai, H., Ye, M., Walker, A.P., Chen, X., 2017. A new process sensitivity index to identify important system processes under process model and parametric uncertainty. Water Resources Research, 53(4): 3476-3490.

Darcy, H.P.G., 1856. Les Fontaines publiques de la ville de Dijon. Exposition et application des principes à suivre et des formules à employer dans les questions de distribution d'eau, etc. V. Dalamont.

Deman, G., Kerrou, J., Benabderrahmane, H., Perrochet, P., 2015. Sensitivity analysis of groundwater lifetime expectancy to hydro-dispersive parameters: the case of ANDRA Meuse/Haute-Marne site. Reliability Engineering & System Safety, 134: 276-286.

Dial, D.C., Sumner, D., 1989. Geohydrology and simulated effects of pumpage on the New Orleans aquifer system at New Orleans, Louisiana. Louisiana Department of Transportation and Development Water Resource Technical Report, 46: 54.

Dial, D.C., Tomaszewski, D.J., 1988. Geohydrology, water quality, and effects of pumpage on the New Orleans aquifer system, northern Jefferson Parish, Louisiana. Water Resources Investigations Report 88-4097. Department of the Interior, U.S. Geological Survey. https://doi.org/10.3133/wri884097

Dirichlet, G.L., 1850. Uber die Reduktion der positiven quadratischen Formen mit drei unbestimmten ganzen Zahlen. J. reine angew. Math., 40: 209.

Duncan, J. M., Brandon, T. L., Wright, S. G., Vroman, N., 2008. Stability of I-walls in New Orleans during hurricane Katrina. Journal of Geotechnical and Geoenvironmental Engineering, 134(5), 681-691. https://doi.org/10.1061/(ASCE)1090-0241(2008)134:5(681)

Dunbar, J.B., Britsch III, L.D., 2008. Geology of the New Orleans area and the canal levee failures. Journal of Geotechnical and Geoenvironmental Engineering, 134(5): 566-582. https://doi.org/10.1061/(ASCE)1090-0241(2008)134:5(566)

Dysart, J. E., Rheaume, S. J., Kontis, A. L., 1999. Induced infiltration from the Rockaway River and water chemistry in a stratified-drift aquifer at Dover, New Jersey, with a section on modeling ground-water flow in the Rockaway River Valley. Water Resources Investigations Report 96-4068, U.S. Geological Survey. https://doi.org/10.3133/wri964068

Eddards, M.L., Kister, L.R., Scarcia, G., 1956. Water resources of the New Oreans area, Louisiana. Circular 374. U.S. Geological Survey. https://doi.org/10.3133/cir374

Ely, D.M., 2006. Analysis of sensitivity of simulated recharge to selected parameters for seven watersheds modeled using the precipitation-runoff modeling system. Scientific Investigations Report 2006-5041: 21. U.S. Geological Survey.

Finch, J., Bradford, R., Hudson, J., 2004. The spatial distribution of groundwater flooding in a chalk catchment in southern England. Hydrological Processes, 18(5): 959-971. https://doi.org/10.1002/hyp.1340

Florian, A., 1992. An efficient sampling scheme: updated latin hypercube sampling. Probabilistic Engineering Mechanics, 7(2): 123-130. https://doi.org/10.1016/0266-8920(92)90015-A

Foged, N. et al., 2014. Large-scale 3-D modeling by integration of resistivity models and borehole data through inversion. Hydrology and Earth System Sciences, 18(11): 4349-4362.

Frazier, D.E., 1967. Recent deltaic deposits of the Mississippi River: their development and chronology. Transaction Gulf Coast Association of Geological Societies, 17: 287-315.

García-Gil, A., Vázquez-Suñé, E., Sánchez-Navarro, J.Á., Lázaro, J.M., Alcaraz, M., 2015. The propagation of complex flood-induced head wavefronts through a heterogeneous alluvial aquifer and its applicability in groundwater flood risk management. Journal of Hydrology, 527: 402-419. https://doi.org/10.1016/j.jhydrol.2015.05.005

Geffray, C. et al., 2019. Verification and validation and uncertainty quantification, Thermal Hydraulics Aspects of Liquid Metal Cooled Nuclear Reactors, 383-405. https://doi.org/10.1016/B978-0-08-101980-1.00008-9

Gotkowitz, M.B., Attig, J.W., McDermott, T., 2014. Groundwater flood of a river terrace in southwest Wisconsin, USA. Hydrogeology Journal, 22(6): 1421-1432. http://dx.doi.org/10.1111/gwat.12373

Green, P.J., Sibson, R., 1978. Computing Dirichlet tessellations in the plane. The Computer Journal, 21(2): 168-173. https://doi.org/10.1093/comjnl/21.2.168

Griffis, F.H., 2007. Engineering failures exposed by Hurricane Katrina. Technology in Society, 29(2): 189-195. https://doi.org/10.1016/j.techsoc.2007.01.015

Heath, R. C., 1998. Basic ground-water hydrology. Water Supply Paper 2220, U.S. Geological Survey. https://doi.org/10.3133/wsp2220

Hele-Shaw, H., 1897. Experiments on the nature of surface resistance in pipes and on ships. Trans. Inst. Naval Archtects, 39: 145-156.

Helton, J.C., Davis, F.J., 2003. Latin hypercube sampling and the propagation of uncertainty in analyses of complex systems. Reliability Engineering & System Safety, 81(1): 23-69.

Hill, M.C., 1998. Methods and guidelines for effective model calibration, Water Resources Investigation Report 98-4005. U.S. Geological Survey. https://doi.org/10.3133/wri984005

Hogan, J., Van der Kamp, G., Barbour, S., Schmidt, R., 2006. Field methods for measuring hydraulic properties of peat deposits. Hydrological Processes, 20(17), 3635-3649. https://doi.org/10.1002/hyp.6379

Hoover, D.J., Odigie, K.O., Swarzenski, P.W., Barnard, P., 2017. Sea-level rise and coastal groundwater inundation and shoaling at select sites in California, USA. Journal of Hydrology: Regional Studies, 11: 234-249. https://doi.org/10.1016/j.ejrh.2015.12.055

Hughes, A. et al., 2011. Flood risk from groundwater: examples from a Chalk catchment in southern England. Journal of Flood Risk Management, 4(3): 143-155. https://doi.org/10.1111/j.1753-318X.2011.01095.x

Huntington, D., Lyrintzis, C., 1998. Improvements to and limitations of Latin hypercube sampling. Probabilistic Engineering Mechanics, 13(4): 245-253. https://doi.org/10.1016/S0266-8920(97)00013-1

ILIT (Independent Levee Investigation Team), 2006. Investigation of the performance of the New Orleans flood protection system in Hurricane Katrina. Retrieved from https://biotech.law.lsu.edu/katrina/ILIT/index.html

Iman, R.L., Conover, W.J., 1980. Small sample sensitivity analysis techniques for computer models, with an application to risk assessment. Communications in Statistics, 9: 1749-1842. https://doi.org/10.1080/03610928008827996

IPET (Interagency Performance Evaluation Team), 2006. Performance evaluation of the New Orleans and Southeast Louisiana hurricane protection system. U.S. Army Corps of Engineers, Washington, D.C. https://lccn.loc.gov/2006618548

Jafari, N.H., Stark, T.D., Leopold, A.L., Merry, S.M., 2015. Three-dimensional levee and floodwall underseepage. Canadian Geotechnical Journal, 53(1): 72-84.

Janetti, E.B., Guadagnini, L., Riva, M., Guadagnini, A., 2019. Global sensitivity analyses of multiple conceptual models with uncertain parameters driving groundwater flow in a regional-scale sedimentary aquifer. Journal of Hydrology, 574: 544-556.

Johnson, A. I., 1967. Specific yield: compilation of specific yields for various materials. Water Supply Paper 1662-D, U.S. Geological Survey. https://doi.org/10.3133/wsp1662D

Jones, C.E. et al., 2016. Anthropogenic and geologic influences on subsidence in the vicinity of New Orleans, Louisiana. Journal of Geophysical Research: Solid Earth, 121(5): 3867-3887. https://doi.org/10.1002/2015JB012636

Kolb, C.R., Smith, F.L., Silva, R.C., 1975. Pleistocene sediments of the New Orleans-Lake Pontchartrain area. U.S. Army Corps of Engineers Technical Report S-75-6, Vicksburg, MS.

Korkmaz, S., Ledoux, E., Önder, H., 2009. Application of the coupled model to the Somme river basin. Journal of Hydrology, 366(1-4): 21-34. https://doi.org/10.1016/j.jhydrol.2008.12.008

Kreibich, H., Thieken, A., Grunenberg, H., Ullrich, K., Sommer, T., 2009. Extent, perception and mitigation of damage due to high groundwater levels in the city of Dresden, Germany. Natural Hazards and Earth System Sciences, 9(4): 1247-1258.

Letts, M.G., Roulet, N.T., Comer, N.T., Skarupa, M.R., Verseghy, D.L., 2000. Parametrization of peatland hydraulic properties for the Canadian Land Surface Scheme. Atmosphere-Ocean, 38(1), 141-160. https://doi.org/10.1080/07055900.2000.9649643

Love, M., Amante, C., Eakins, B., Taylor, L., 2010, Digital elevation models of New Orleans, Louisiana: Procedures, data sources and analysis. National Geophysical Data Center, Marine Geology and Geophysics Division, Boulder, Colorado.

Macdonald, D. et al., 2008. Improving the understanding of the risk from groundwater flooding in the UK. Proceedings of the European Conference on Flood Risk Management, Oxford. http://nora.nerc.ac.uk/id/eprint/7760

Macdonald, D., Dixon, A., Newell, A., Hallaways, A., 2012. Groundwater flooding within an urbanised flood plain. Journal of Flood Risk Management, 5(1): 68-80. https://doi.org/10.1111/j.1753-318X.2011.01127.x

Mansur, C.I., Postol, G., Salley, J.R., 2000. Performance of relief well systems along Mississippi River levees. Journal of Geotechnical and Geoenvironmental Engineering, 126(8): 727-738.

MathWorks, 2015. Optimization Toolbox: User's Guide. Retrieved from https://www.mathworks.com/help/optim/index.html

McDonald, M.G., Harbaugh, A.W., 1988. A modular three-dimensional finite-difference ground-water flow model. Techniques of Water Resources Investigations 06-A1, U.S. Geological Survey Reston, VA. https://doi.org/10.3133/twri06A1

McGlynn, B.L., McDonnell, J.J., Seibert, J., Kendall, C., 2004. Scale effects on headwater catchment runoff timing, flow sources, and groundwater-streamflow relations. Water Resources Research, 40(7). https://doi.org/10.1029/2003WR002494

McKay, M.D., 1992. Latin hypercube sampling as a tool in uncertainty analysis of computer models. Proceedings of the 1992 Winter Simulation Conference, 557-564. https://doi.org/10.1145/167293.167637

Metya, S., Mukhopadhyay, T., Adhikari, S., Bhattacharya, G., 2017. Efficient system reliability analysis of earth slopes based on support vector machine regression model, Handbook of Neural Computation. Elsevier, 127-143. https://doi.org/10.1016/B978-0-12-811318-9.00007-7

Morris, S., Cobby, D., Zaidman, M., Fisher, K., 2018. Modelling and mapping groundwater flooding at the ground surface in Chalk catchments. Journal of Flood Risk Management, 11: S251-S268. https://doi.org/10.1111/jfr3.12201

Négrel, P., Petelet-Giraud, E., 2005. Strontium isotopes as tracers of groundwater-induced floods: the Somme case study (France). Journal of Hydrology, 305(1-4): 99-119.

Negri, S., Leucci, G., Mazzone, F., 2008. High resolution 3D ERT to help GPR data interpretation for researching archaeological items in a geologically complex subsurface. Journal of Applied Geophysics, 65(3-4): 111-120.

Nocedal, J., Wright, S.J., 2006. Numerical Optimization, Springer, New York. https://doi.org/10.1007/978-0-387-40065-5

Panday et al., 2013. MODFLOW-USG version 1: An unstructured grid version of MODFLOW for simulating groundwater flow and tightly coupled processes using a control volume

finite-difference formulation: U.S. Geological Survey Techniques and Methods, book 6, chap. A45, 66 p. Retrieved from: https://pubs.usgs.gov/tm/06/a45

Panday et al., 2017. MODFLOW-USG version 1.4.00: An unstructured grid version of MODFLOW for simulating groundwater flow and tightly coupled processes using a control volume finite-difference formulation: U.S. Geological Survey Software Release, 27 October 2017. https://dx.doi.org/10.5066/F7R20ZFJ

Pinault, J.L., Amraoui, N., Golaz, C., 2005. Groundwater-induced flooding in macropore-dominated hydrological system in the context of climate changes. Water Resources Research, 41(5).

Poeter, E., Hill, M., 1997. Inverse models: a necessary next step in groundwater modeling. Groundwater, 35 (2): 250–260.

Prickett, T.A., 1975. Modeling techniques for groundwater evaluation. Advances in Hydroscience, 10: 1-143. https://doi.org/10.1016/B978-0-12-021810-3.50006-0

Rain, D., Engstrom, R., Ludlow, C., Antos, S., 2011. Accra Ghana: a city vulnerable to flooding and drought-induced migration. Global Report on Human Settlements, May, 21.

Rajabi, M.M., Ataie-Ashtiani, B., Simmons, C.T., 2015. Polynomial chaos expansions for uncertainty propagation and moment independent sensitivity analysis of seawater intrusion simulations. Journal of Hydrology, 520: 101-122.

Rosenzweig, C. et al., 2011. Developing coastal adaptation to climate change in the New York City infrastructure-shed: process, approach, tools, and strategies. Climatic Change, 106(1): 93-127. http://dx.doi.org/10.1016/j.jclepro.2015.05.045

Rotzoll, K., Fletcher, C.H., 2013. Assessment of groundwater inundation as a consequence of sea-level rise. Nature Climate Change, 3(5): 477-481. https://doi.org/10.1038/nclimate1725

Saltelli, A., Tarantola, S., Chan, K.-S., 1999. A quantitative model-independent method for global sensitivity analysis of model output. Technometrics, 41(1): 39-56.

Samaras, E., Shinozuka, M., Tsurui, A., 1985. ARMA representation of random processes. Journal of Engineering Mechanics, 111: 449-461.

Saucier, R.T., 1963. Recent geomorphic history of the Pontchartrain Basin, Louisiana. Technical Report No. 16, United States Gulf Coastal Studies, Coastal Studies Institute, Contribution No. 63-2, Louisiana State University, Baton Rouge, LA.

Seed, R.B. et al., 2008a. New Orleans and Hurricane Katrina. I: Introduction, overview, and the east flank. Journal of Geotechnical and Geoenvironmental Engineering, 134(5): 701-717. https://doi.org/10.1061/(ASCE)1090-0241(2008)134:5(701)

Seed, R.B. et al., 2008b. New Orleans and Hurricane Katrina. IV: Orleans east bank (metro) protected basin. Journal of Geotechnical and Geoenvironmental Engineering, 134(5): 762-779. https://doi.org/10.1061/(ASCE)1090-0241(2008)134:5(762)

Seed, R.B. et al., 2008c. New Orleans and Hurricane Katrina. II: the central region and the lower Ninth Ward. Journal of Geotechnical and Geoenvironmental Engineering, 134(5): 718-739. https://doi.org/10.1061/(ASCE)1090-0241(2008)134:5(718)

Seed, R.B. et al., 2008d. New Orleans and hurricane Katrina. III: The 17th street drainage canal. Journal of Geotechnical and Geoenvironmental Engineering, 134(5): 740-761. https://doi.org/10.1061/(ASCE)1090-0241(2008)134:5(740)

Sherard, J.L., 1963. Earth and Earth-Rock Dams. John Wiley and Sons, New York.

Shinozuka, M., Deodatis, G., 1991. Simulation of stochastic processes by spectral representation. Applied Mechanics Review, 44: 191-204.

Sibson, R., 1980. A vector identity for the Dirichlet tessellation. Mathematical Proceeding of the Cambridge Philosophical Society, 87(1): 151-155. https://doi.org/10.1017/S0305004100056589

Sibson, R., 1981. A brief description of natural neighbour interpolation. V. Barnett (Ed.), Interpreting Multivariate Data, John Wiley and Sons, New York.

Slooten, L.J., Carrera, J., Castro, E., Fernandez-Garcia, D., 2010. A sensitivity analysis of tide-induced head fluctuations in coastal aquifers. Journal of Hydrology, 393(3-4): 370-380.

Snowden, J.O., Ward, W.C., Studlick, J.R.J., 1980. Geology of greater New Orleans: Its relationship to land subsidence and flooding. The New Orleans Geological Society, New Orleans, LA.

Stark, T.D., Jafari, N.H., Leopold, A.L., Brandon, T.L., 2014. Soil compressibility in transient unsaturated seepage analyses. Canadian Geotechnical Journal, 51(8): 858-868. https://doi.org/10.1139/cgj-2013-0255

Thangarajan, M., 2007. Groundwater models and their role in assessment and management of groundwater resources and pollution, in: Thangarajan, M. (Ed.), Groundwater Resource Evaluation, Augmentation, Contamination, Restoration, Modeling and Management. Capital Publishing Company, New Delhi, India.

Tsai, F.T.-C., Sun, N.Z., Yeh, W.W.-G., 2005. Geophysical parameterization and parameter structure identification using natural neighbors in groundwater inverse problems. Journal of Hydrology, 308(1): 267-283.

Turner, A.K., 2006. Challenges and trends for geological modelling and visualisation. Bulletin of Engineering Geology and the Environment, 65(2): 109-127.

Upton, K., Jackson, C., 2011. Simulation of the spatio-temporal extent of groundwater flooding using statistical methods of hydrograph classification and lumped parameter models. Hydrological Processes, 25(12): 1949-1963. https://doi.org/10.1002/hyp.7951

USACE (U.S. Army Corps of Engineers), 1956. Investigation of underseepage and its control, lower Mississippi River levees." Technical Memorandum TM 3-424, USACE Mississippi River Commission Waterways Experiment Station, Vicksburg, MS.

USACE (U.S. Army Corps of Engineers), 1992. Design, construction, and maintenance of relief wells. Engineering Manual EM 1110-2-1914, Washington, D.C.

Visocky, A.P., 1995. Determination of 100-year ground-water flood danger zones for the Havana and Bath areas, Mason County, Illinois. Illinois State Water Survey Contract Report CR-584, Champaign, Illinois.

Voronoi, G., 1908. Nouvelles applications des paramètres continus à la théorie des formes quadratiques. Premier mémoire. Sur quelques propriétés des formes quadratiques positives parfaites. Journal für die reine und angewandte Mathematik (Crelles Journal), 1908(133): 97-102.

Wolff, T.F., 1989. Levee underseepage analysis for special foundation conditions. Technical Report REMR-GT-11, U.S. Army Corps of Engineers, Washington D.C.

Yin, J. et al., 2011. Multiple scenario analyses forecasting the confounding impacts of sea level rise and tides from storm induced coastal flooding in the city of Shanghai, China. Environmental Earth Sciences, 63: 407-414. https://doi.org/10.1007/s12665-010-0787-9

Younger, P., 1993. Simple generalized methods for estimating aquifer storage parameters. Quarterly Journal of Engineering Geology and Hydrogeology, 26(2), 127-135. https://doi.org/10.1144/GSL.QJEG.1993.026.02.04

Zeng, X., Wang, D., Wu, J., 2012. Sensitivity analysis of the probability distribution of groundwater level series based on information entropy. Stochastic Environmental Research and Risk Assessment, 26(3): 345-356.

Zope, P.E., Eldho, T.I., Jothiprakash, V., 2015. Impacts of urbanization on flooding of a coastal urban catchment: a case study of Mumbai City, India. Natural Hazards, 75: 887-908. https://doi.org/10.1007/s11069-014-1356-4

Vita

Shuo Yang received his bachelor's degree in the Department of Hydrology at Jilin University. Then he was enrolled in the master program in Civil and Environmental Engineering Department with the specialization of water resource engineering at Louisiana State University, Baton Rouge. He worked as a research assistant in the program. He anticipates graduating with a master's degree in May 2020.